12-2019

# Development of fluidic devices for use in Transient Absorption Microscopy towards the study of Amphotericin B

Brandon Woitas
*University of Tennessee*, bwoitas@vols.utk.edu

To the Graduate Council:

I am submitting herewith a thesis written by Brandon Woitas entitled "Development of fluidic devices for use in Transient Absorption Microscopy towards the study of Amphotericin B." I have examined the final electronic copy of this thesis for form and content and recommend that it be accepted in partial fulfillment of the requirements for the degree of Master of Science, with a major in Chemistry.

Tessa R. Calhoun, Major Professor

We have read this thesis and recommend its acceptance:

Michael Best, Bhavya Sharma

Accepted for the Council:
Dixie L. Thompson

Vice Provost and Dean of the Graduate School

(Original signatures are on file with official student records.)

# Development of fluidic devices for use in Transient Absorption Microscopy towards the study of Amphotericin B

A Thesis Presented for the

Master of Science

Degree

The University of Tennessee, Knoxville

Brandon Matthew Woitas

December 2019

*To my family and friends, without you, none of this would be possible, thank you for your never ending love and support...*

# Acknowledgments

First, thank you to my advisor, Dr. Tessa Calhoun, for your support and guidance throughout my time here at UTK. Thank you for always having an open door for any questions, concerns, or just to chat. Thank you for all of the experience and knowledge I have gained in this field during my time here.

Thank you to my fellow past and present group members, Lindsey, Brandon C., Redwan, Kevin M., Kevin H., and Brianna W., who were always around to deal with my silly questions, listen to my frustrations, and most importantly, gossip.

Lastly, thank you to my committee members, Dr. Michael Best and Dr. Bhavya Sharma for your time and dedication to my success.

# Abstract

Flow cell devices have been used extensively in microscopy. Here, we present a new development of fluidic devices that can be used with high resolution transient absorption microscopy in the observation of ultrafast dynamics of solutions, and most importantly, drug-membrane interactions. The evolution of the flow cell devices will be discussed along with their applications in the study of an antifungal drug, Amphotericin B (AmB). The study of AmB with transient absorption microscopy in solution, living systems, and its recent progress on discovering the underlying mechanism of action label-free will be presented. It is discovered that AmB's interaction with membranes may be sensitive to environmental factors, and that changing conditions may affect its mechanism of action. Commercial Fungizone® solution is also explored and discovered to give different dynamics in solution over monomeric AmB. Overall, the applications, developments, and improvements of the flow cell devices, along with the recent studies on AmB and Fungizone will be discussed.

# Table of Contents

# List of Tables

# List of Figures

# Chapter 1

# Introduction

## 1.1 Motivation

Fluidic devices in microscopy are common, however, are most extensively used in bright field microscopy and uncommon in transient absorption. This is due to the fact that commercialized fluidic cell devices are designed to be used on an inverted microscope with viewing on only one side of the chamber with a single objective, designed for one-time use, and are not concerned with sterility or adhesion of living systems. These devices are called "flow cells." To use these devices in transient absorption, a new design of a flow cell was needed to run our experiments. Our TAM instrument requires a glass-to-glass flow cell in where we can focus two high-NA objectives onto the sample, flow our solutions, and sterilize and functionalize glass for immobilization of living systems, if needed. We began with an all-glass flow cell device that checked all of the boxes for our requirements for our studies. This device was then optimized and evolved into an all-plastic design that is robust and built for long-term use. The evolution and design of these flow cell devices will be discussed in detail in chapter 2.

One of the most significant reasons why the flow cell devices were developed, was to study a novel antifungal drug, Amphotericin B. Amphotericin B (AmB), is a polyene-class antifungal that has been around for over 50 years with very limited amount of resistance shown.[60] However, with it brings harmful side effects to the patient causing death in the rarest cases. Therefore, it is only used in the most severe life-threatening fungal infections.

Even while AmB has been in existence for such a long period of time, the exact mechanism of action (MOA) is still unknown to this date. Over the years, many mechanisms have been proposed in the literature with no ultimate conclusion of how the drug is causing cell death in fungi.[24, 59, 3] This lack of understanding limits a more targeted approach in the design of an improved version of the drug. To understand the interaction that this drug may be having with the living system, traditional microscopy studies would involve the addition of a bulky fluorescent probe, due to AmB being naturally non-fluorescent and demonstrating a low quantum yield. With the addition of this probe, the natural interaction of AmB with the fungi can be altered.[10, 31] However, due to the polyene backbone present in the molecular structure of AmB, we can study the drug label-free with transient absorption microscopy (TAM). AmB is a strong absorber of light, which is all that is required for the use of this technique. The previous and recent results on the study of AmB with TAM will be discussed in chapter 3. Later on, we also explored commercial Fungizone ® solution which is discussed in chapter 4.

## 1.2 Transient Absorption Microscopy

Transient absorption microscopy (TAM) is a nonlinear optical technique that can provide diffraction limited resolution spatially and femtosecond resolution temporally, by focusing ultrafast laser pulses through high-NA objectives. The high-NA objectives are necessary to obtain a tight-focus onto the sample, and to achieve the best resolution possible.[25] This technique bases its contrast on nonlinear interactions of light with matter.[22] Two ultrafast laser pulses, which are referred to as the "pump" and "probe" are focused down onto the sample and overlapped in space. The pump pulse arrives at the sample first and excites the sample. The probe pulse then follows at a known time delay on a femtosecond (fs) time scale ($10^{-15}$), to further interact with the sample. Our TAM consists of a mode-locked Ti:sapphire laser oscillator which produces pulses of ∼80 fs at a repetition rate of 80 MHz. Laser systems with a high-repetition rate are the best for TAM experiments because they give high pulse energies and can reduce noise.[64] A schematic of our system can be seen in Fig 1.1.

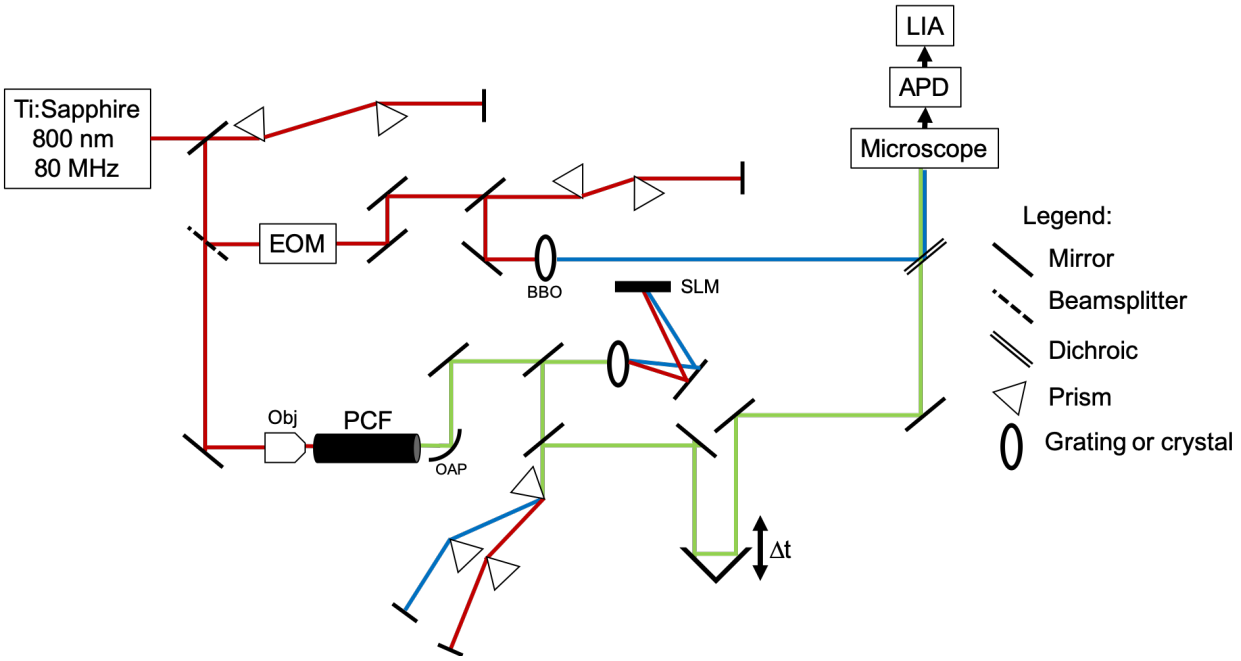


**Figure 1.1:** Schematic of our TAM setup. EOM = electro-optic modulator, Obj = objective, PCF = photonic crystal fiber, OAP = off-axis parabolic mirror, SLM = spatial light modulator, BBO = $\beta$-barium borate crystal, APD = avalanche photodiode, LIA = lock-in amplifier.

### 1.2.1 Instrumentation

The laser produces an output centered around 800 nm but contains 12 nm of bandwidth. To compress this light the output from the oscillator is first sent through a prism pair to correct for any dispersion and to ultimately have our pulses as compressed as possible for the photonic crystal fiber device (PCF). Then, this beam is split into two beams, the pump and probe.

#### Dispersion

Dispersion is introduced to the system when traveling through different materials and optics, where the pulses can get broadened and dispersed in time. We have different optics in place to correct for different orders of dispersion that are introduced into the system. Prism lines on the table correct for second and third order of dispersion where second order dispersion the pulse is delayed with respect to wavelength, and third order dispersion results in pulse

propagation. The spatial light modulator (SLM), which will be discussed in the "Probe" section of 1.2.1 also corrects for higher order dispersion in our system.

### Pump

The pump beam is modulated at 26.66 MHz with an electro-optic modulator (EOM) for detection with our lock-in amplifier (LIA), which can isolate signal from our samples at this specific frequency. The EOM operates by taking the reference frequency and "pulse picking" the signal at that same frequency from the input. The EOM is set to pick every third pulse, which sets the repetition rate to be divided by three which represents the 26.66 MHz respectively. From here, the pump beam is then sent through a second prism compression pair to obtain optimal efficiency through a second harmonic generating (SHG) crystal. In this setup, we are using a $\beta$-barium borate (BBO) crystal to frequency-double the 800 nm output of the oscillator to 400 nm for our Amphotericin B studies. We also have the option of removing the crystal to pump the sample with 800 nm light, which we also use for compression methods on our microscope such as second harmonic generation frequency resolved optical gating (SHG-FROG), co-linear-FROG (cFROG), and cross correlation-FROG (xFROG).[2, 43, 25]

### Probe

The probe beam gets sent through a photonic crystal fiber (PCF) which generates supercontinuum white light. The dispersive wave is controlled by a power attenuator consisting of a polarizer and a $\lambda/2$ waveplate (not shown). The dispersive wave is characterized by the most blue-shifted wavelength emitted by the PCF fiber spectrum and can be seen in Fig 1.2.[4]

The probe beam then goes through a spatial light modulator (SLM) to correct higher order dispersion that is introduced by the PCF.[37, 34] Since we are producing a white light spectrum, dispersion is also introduced by the PCF which separates the different wavelengths that compose the white light in time. In order to align all of the wavelengths in time, the pulse shaping line consisting of the SLM is used, which has been described previously in detail.[19] The SLM is composed of a liquid crystal display (LCD) pixel array that changes

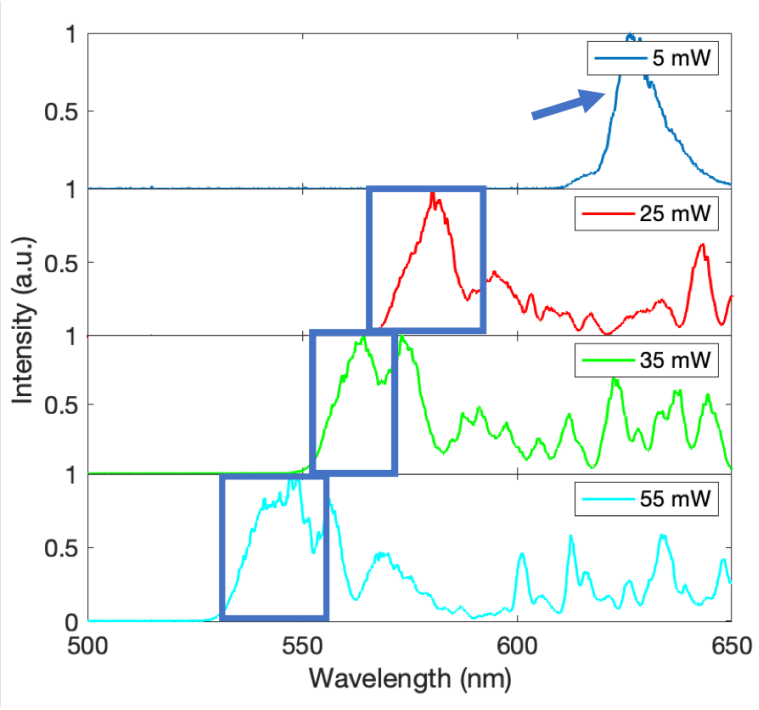


**Figure 1.2:** Spectra of Femtowhite 800 fiber output with varying 800 nm laser power input. The dispersive wave is pointed to in the 5mW spectra and boxed in blue in the following spectra.

the refractive index of each pixel that corresponds to each wavelength of light to match them all in time.[21, 63] From here, to further compress the probe, the beam is sent through a prism compression pair. The prism compression pair is necessary because the SLM-based compression line is only able to correct for higher orders of dispersion. Once the beam leaves the SLM line, the prism line is in place to correct for any second-order dispersion that remains. The SLM and prism compression line has been previously confirmed to be beneficial to our studies.[36] The probe light reaches a retroreflector time delay stage, which is controlled from the data collection computer via software codes written in LabVIEW.

### Recombination into the microscope

Then the probe beam is recombined with the pump beam, and both of the beams are focused through a 1.4 NA objective. The sample is placed on a piezo stage which allows for x-, y-, and z-scanning of samples for imaging. After hitting the sample, the beams are collected with a second 1.4 NA objective. Based on our probe wavelength and the high-NA objectives, using

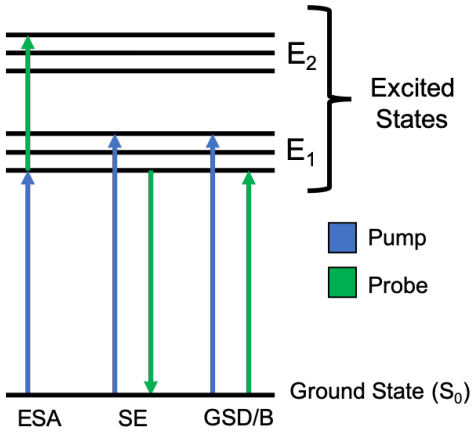


**Figure 1.3:** Energy diagram showing major processes in transient absorption microscopy. Excited-state absorption (ESA), Stimulated Emission (SE), and Ground-State Depletion/Bleach (GSD/B)

resolution equations 1.1 and 1.2, respectively, we can obtain a lateral resolution of ~220 nm and an axial resolution of ~525 nm.[22] Where $\lambda$ is our probe wavelength of 550 nm, $n$ is the refractive index of our immersion oil (n=1.518) and NA in all cases is 1.4.

$$R_{lateral} = \frac{0.54\lambda}{NA^{0.91}} \tag{1.1}$$

$$R_{axial} = \frac{0.89\lambda}{n - \sqrt{n^2 - NA^2}} \tag{1.2}$$

The stronger pump beam is then filtered out with a 450 nm long pass filter. The TA signal is detected by an avalanche photodiode (APD), which was selected for use due to its high sensitivity and response time.[33] The APD is connected to the LIA which isolates signal changes at the frequency that is referenced from the EOM (pump line). The lock-in essentially filters out the signal at this frequency, and then amplifies it.[57] This is to filter out any background signal by our un-modulated probe beam, and to collect signal coming from an interaction with the sample. By varying the known time delay ($\tau$) between the pump and probe pulse, we can then record this change in absorption/signal ($\Delta$A). The response can then be plotted as a function of the time delay $\tau$ and the intensity. From here, we can then learn about multiple dynamic processes that occur.[8] Major processes that occur when these laser pulses interact with a sample include excited-state absorption, stimulated emission, and ground-state depletion/bleach as can be seen in Fig 1.3.[8]

## 1.3 Amphotericin B

Amphotericin B has been around for over 50 years helping patients who require treatment from life threatening fungal infections.[60] This medication is important because fungal infections are a serious threat to society causing an estimated one million deaths worldwide per year.[16] Despite advances in the synthesis of modern medicine, the mortality rate for fungal infections is still rising.[11] The underlying issue of the severity of fungal infections is the resistance growing against these medications. Antifungal resistance is where fungi develop the ability to alter their responsivity to these medications and can quickly become resistant to new drugs that are being developed.[45, 40]

Amphotericin B (AmB) is a very effective antifungal that has shown limited amounts of resistance over its lifetime but has a plethora of unpleasant side effects leading up to death.[50] Due to these lethal side effects, AmB is most often used as a patient's "last resort" for survival.[6] Because of the harmful outcomes of AmB, different formulations have been developed to lessen the toxicity of the drug. These include an AmB lipid complex (ribbon-like structures), AmB colloidal dispersion (disc-like structures), and liposomal AmB (liposome structure).[5, 28] These formulations of phospholipid carriers are great for reducing the risk of mortality and toxicity; however, higher doses of these formulations must be given to the patient because the efficacy of the drug has now decreased severalfold.[20] To help alleviate the side effects or implement AmB's power into new drug formulations, it is crucial to gain a better understanding of how AmB acts with fungi on the molecular level. AmB has been proposed to interact with the fungal cells in three unique mechanisms as shown in Fig 1.4. In the first mechanism (a), the drug binds to ergosterol and forms a "pore/ion channel" where essential cations ($K^+$, $Ca^{2+}$, etc.) leak across the membrane and flow out of the cell causing it to die.[24] In the second proposed mechanism (b), AmB is internalized into the cell and induces the accumulation of radical oxygen species causing cell death.[59] The third mechanism (c) is proposed to happen by the drug aligning itself parallel to the outer layer of the membrane and acting as a "sterol sponge," seizing ergosterol and then destabilizing the cell membrane leading to death.[3]

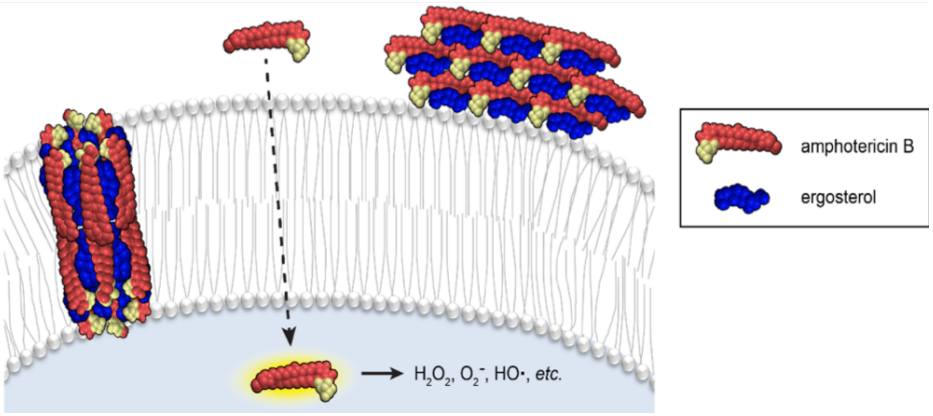


**Figure 1.4:** Model of the three proposed mechanisms for AmB, (a) "pore/ion channel" mechanism, (b) intracellular accumulation of reactive oxygen species, (c) "sterol sponge", ergosterol sequestration

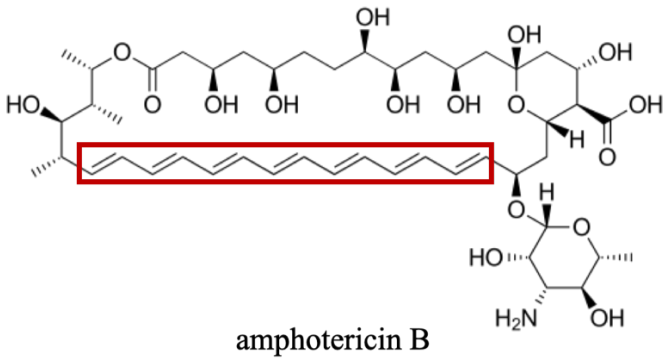


**Figure 1.5:** Structure of Amphotericin B with the chromophore highlighted in red

To complete a traditional fluorescence microscopy study of AmB, a fluorescent probe is added to the drug as it is weakly fluorescent.[10, 31] The addition of fluorescent labels to AmB has been shown to be disruptive to the original molecule, especially in small molecules such as AmB where the fluorescent label is often larger than the molecule itself.[53] There are also concerns of the probe interfering with the natural mechanism-of-action (MOA). For example, a study by Zumbuehl et al., has demonstrated an Amphotericin B-Fluorescein conjugate which can be fluorescently detected, yet has shown to completely lack toxic effects on yeast cell growth.[67]

However, AmB is a polyene antifungal and contains a chromophore as shown in Fig 1.5, which is different from other common antifungals such as flucytosine, which is a cyclic-type antifungal.[62] Because of this polyene, and because TAM only requires the molecule of interest to absorb light, we can use TAM to study this distinctive antifungal label-free. This

is one of the many advantages of using TAM over traditional fluorescence which would use a bulky-probe attached to AmB. The advantages of using TAM include the ability to non-destructively monitor AmB label-free, and excellent spatial and temporal resolution due to the use of high-NA objectives in our instrument. Results have already been obtained with our instrument using AmB in solution both in its monomeric state and aggregated state, and imaging studies have been attempted. In this thesis, studies on observing excited state dynamics of Amphotericin B in solution and attempts to image its drug-membrane interactions with living and model systems will be discussed in Chapter 3.

# Chapter 2

# Flow Cell Devices

## 2.1 Introduction

Transient absorption microscopy as previously mentioned, involves focusing two ultrafast laser pulses of light onto a sample. To do this, especially with a liquid solution, an apparatus is needed to maintain the liquid in solution for the time being while it is over the sample position on our microscope. These apparatuses are commonly known as "flow cells," and commonly consist of a chamber or channel where the solution is present, ports for flowing, and then an area where it can be viewed on a microscope. Flow cell devices are often used in microscopy; however, commercially available flow cell devices are not compatible for the types of experiments that we carry out in our lab. For our studies and experiments, we needed a flow cell device that had the following qualities:

1. Maintained the liquid in solution and could be flowed over the focal spot
2. Allowed for high-NA objectives with a small working distance to be used
3. Can be sterilized and functionalized for living system studies
4. Was inexpensive and can be used multiple times

We required the solution to be flowing over the focal spot of our system due to photobleaching. If we had a static solution sitting over our focal spot, over time the

sample will result in photobleaching and ultimately reduced signal and unreliable data. Photobleaching of a sample is when the sample has been exhausted of its capabilities to interact with light.[52] The molecule succumbs to photon-induced chemical damage and will no longer give off signal. Published evidence has shown that photobleaching is more rapid under two-photon excitation rather than traditional one-photon microscopy, and is why this is of importance to us.[56] There is also a concern of thermal issues when observing a liquid sample, and a static sample could be drying out in the chamber or being altered by the heat of the laser being focused on one spot for a long period of time. The flow of the solution will combat both of these issues. Using two high-NA objectives requires space for the objectives to focus due to the small working distance ($\sim 0.26$ mm), along with thin coverglass-to-coverglass—not offered by any commercial manufacturer. Other types of commercially available flow cell devices were used in our lab but were shown to give off background signals that are intrusive to our studies. They also were not made to be observed on both sides, one side was cover glass, but the other was a plastic material such as polycarbonate.[51] For example, the Ibidi ® sticky-Slide Luer product was the first commercial flow cell device to be tested. The top piece of the flow cell was made out of a material that the company would not disclose, but it was assumed to be some type of plastic material as it was disclosed to melt at 140° F. This also prohibited us from autoclaving the device to maintain sterility for our living system studies. The underside of this slide was "sticky" and contained an adhesive to attach a thin-coverglass to finish the channel. The device did flow properly, however the adhesive was also unknown to us and could not be validated it would not disintegrate with solvents. The ultimate reason why these did not succeed, was the background signal that was obtained from the "plastic" top part of the device. The device itself gave off transient absorption signal even when no solution was present. This commercial device was also quite thick, and at the time we were not using as high of a numerical aperture for our objectives, so this was not an issue. To overcome the issues of the working distances of our high-NA objectives an all-glass coverslip-to-coverslip flow cell device was designed and will be discussed in detail in section 2.3.1. A schematic of this device can be seen in Fig 2.1 and in Fig 2.2. This flow cell has a cut-out specifically for our objectives to allow for the 0.26 mm working distance between them. The third reasoning of why we created our own device was

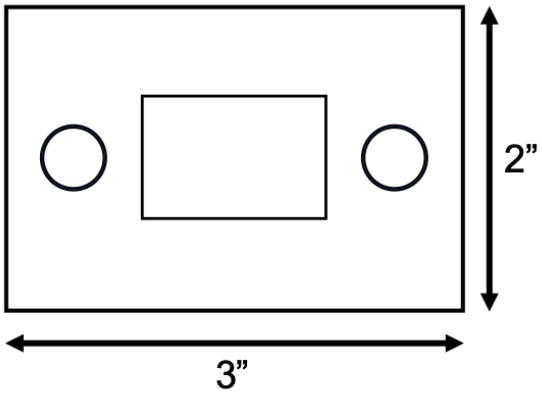


**Figure 2.1:** Glass Flow Cell

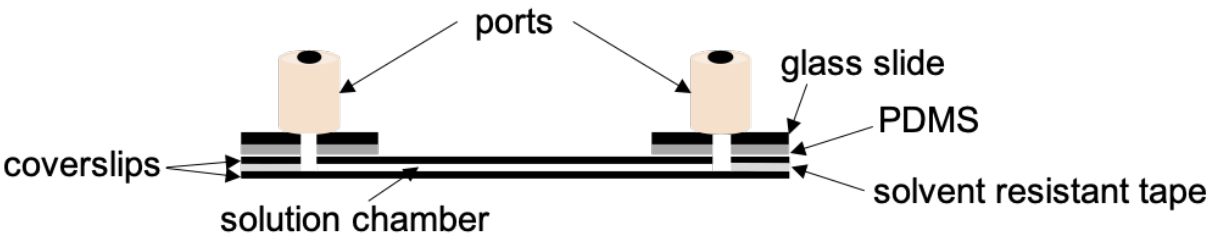


**Figure 2.2:** Side View of Glass Flow Cell

due to the living systems we study. In order to use the devices for living systems, we need to maintain sterility of all components, along with the capability to functionalize the glass where the cells will be placed to immobilize them. With the glass device we designed, we can ethanol sterilize the glass base of the device, and then place an autoclaved and functionalized coverglass over containing the immobilized cells and continue with the experiment. After use, the coverglass can be removed from the supporting glass and be disposed of properly in biological waste, and the supporting glass can be bleached and rinsed with ethanol. The last and final reason why we developed our own device, was due to cost. The commercial devices available through Ibidi® are one-time use due to the adhesive and are only available as a pack of 15 and cost $240 per pack. We can produce our own glass devices for a fraction of the cost due to the reusability of the devices and the parts used to produce them over time.

## 2.2 Motivation

Once developed, we planned to use these devices in a variety of ways. One way and the most commonly used to this date on our lab, is to observe dynamics of molecules. We do this by flowing a solution through our flow cell device, using a syringe pump to control the flow, and placing the flow cell onto the microscope stage and securing with double-sided tape for use. We also use the device for pump pulse compression and for flowing drugs over living and model systems for observing drug-membrane interactions when imaging the respective systems. Down the road, this all-glass flow cell system lead to daily breaking and ultimately lots of down time in the lab and more time spent making the devices than actually using them. This led us to design a more permanent device to be used. The more permanent device is machined by our in-house machine shop out of Delrin material, and is re-usable, saving much time in the lab. Details about each type of cell will be described in section 2.3.

## 2.3 Devices

### 2.3.1 Glass Flow Cell

With the help of Dr. Christopher Baker in the UTK chemistry department, the glass flow cell was designed to have a cut out for our high-NA objectives, two ports (sample inlet and outlet) for flow, a glass-to-glass design for the solution, and a polydimethylsiloxane (PDMS) layer between the supporting glass slide and the first glass coverslip layer in order to bond the pieces together and add support. The glass parts were purchased from Fisher Scientific, the ports were purchased from IDEX, Inc. and the PDMS from Stockwell Elastomerics. The corresponding part numbers for the components are listed in Table 2.1.

These components remained consistent throughout the usage of the glass flow cell devices in the lab and were used to make many glass flow cell devices over the course of a few months until the time-consuming process became a productivity issue. The procedure of how the glass device was made can be seen below. In short, it consists of a 2" × 3" glass microscope slide, a layer of PDMS to bond the glass together, then a 2" × 3" coverglass piece.

**Table 2.1:** Glass Flow Cell Components

| Component | Description | Vendor | Item Number |
|---|---|---|---|
| Glass | 2" × 3" Plain Glass Microslides | Fisher Scientific | 12-550C |
| Coverslip | Ted Pella Inc Coverglass 2" × 3" | Fisher Scientific | NC0279614 |
| PDMS | 0.010" thick liquid silicone | Stockwell Elastomerics | HT6240 |
| Ports | NanoPort Assembly | IDEX, Inc | N-333 |
| Silicone | Clear Silicone Waterproof Sealant | Loctite | 908570 |

### Procedure for Glass Flow Cell

1. A Dremel® drill device was used with the Flex-Shaft attachment to free-hand cut out the square in the middle of the 2"×3" supporting glass side layer which is submerged in a water bath after an outline was traced. This is shown in Fig 2.3[1]. This cut-out is important, as this is where our collection objective is allowed to focus down onto the sample flowing.

2. The cut slides are then rinsed with deionized (DI) water and then placed in a 250-mL beaker along with the large glass coverslips and then covered completely with 190-proof ethanol (Decon™ Labs). The cut slides are shown in Fig 2.3[2]

3. After submersion, the supporting glass slides and the coverslips are placed in a sonicator bath under the 190-proof ethanol at 40kHz and sonicated for five minutes. The bath can be seen in Fig 2.3[3]

4. After sonication, the glass and coverslips are rinsed quickly with acetone and isopropyl alcohol and are blown dry with nitrogen until spot and dust free. The process can be seen in Fig 2.3[4]. This step is to ensure the glass is free of any organic residue and is completely clean and ready for plasma bonding. If this step was not followed thoroughly the glass would not be clean enough to bond to the PDMS properly and result in a weakly formed flow cell device.

5. The PDMS was cut to a 2" × 3" rectangle to fit the glass from a sheet roll The first protective layer is peeled off and placed facing up, along with the glass slide into a plasma cleaner (Harrick Plasma PDC-001-HP) set to "HI" and was let to "clean" for

approximately five minutes. The inside of the plasma chamber along with the cut glass and PDMS can be seen in Fig 2.4[5].

6. After cleaning, the PDMS and the glass slide were placed together, and gentle pressure was applied ensuring contact between all places was made. Note the upper right corner of Fig 2.4[6] where pressure has not been applied yet and there is still bonding needed, while in in the lower left corner the pieces become clear once bonded.

7. The bonded piece was then placed on a hot plate set to 80° C for five minutes. This is to ensure the bond sets properly and any air bubbles dissipate out. This process is shown in Fig 2.4[7].

8. After cooling, the inner square and any excess PDMS was cut with a razor blade and removed. This step is shown in Fig 2.4[8]. Caution is to be taken when removing the inner square to not scrape or break the glass when removing the inner PDMS.

9. The remaining protective layer on the PDMS is removed and placed face up along with the coverslip in the plasma cleaner chamber and cleaned on "HI" for five minutes. This is shown in Fig 2.5[9], the purple glow is from the plasma cleaner when it is set to the "on" position.

10. The same procedure was followed in regard to gentle pressure and placing the bonded piece on the hot plate as shown in Fig 2.5[10].

11. Two holes were then drilled approximately 1/4" away from the square on both sides through all layers of glass with an 80-grit diamond coated 1/16" bit. This step is shown in Fig 2.5[11]. This is to allow the ports to be placed and for the solution to flow through the chamber.

12. Once the holes are drilled, the ports were then centered and hand-siliconed onto the supporting glass slide with quick grip clamps and let to cure overnight. This is shown in Fig 2.5[12]. We use silicone instead of epoxy, which is more commonly used, because silicone is more solvent resistant for our uses. DMSO will dissolve epoxy and we use

this solvent quite often. Once cured, the flow cell is now ready for the final piece of 1" × 3" coverglass.

13. A flow channel is cut from solvent resistant tape listed in Table 2.2 by a Cricut® device. The channel can be customized for the study, but most traditionally we use a single channel 2.25" by 0.25". Shown in Fig 2.6[13].

14. Once cut, this channel is centered on the ports of the large glass flow cell base and gentle pressure is applied to adhere the first layer of the double sided solvent resistant tape. Shown in Fig 2.6[14].

15. The second protective layer of the solvent resistant tape is removed [A] and the 1" × 3" coverglass is applied over the tape layer and gentle pressure is applied again to adhere the coverglass [B]. Shown in Fig 2.6[15A] and [15B].

When ready to use, the microfluidic tubing is screwed into the siliconed ports with parts from IDEX, Inc. listed in Table 2.2 and the flow cell is attached to the microscope stage with 3M™ double-sided tape and is ready to flow solution. A schematic of the flow cell can be seen in Fig 2.1 and Fig 2.2. After use, nitrogen gas is used to dry any remaining solvent in the flow channel. The tubing and connectors removed, and the glass is placed in a soapy water bath on a hot plate set to 80° C for a few minutes to allow the adhesive to loosen. This is to ensure the final coverslip is loosened enough, to lessen damage to the bonded coverslip. After soaking, the final coverslip is carefully removed with a razor blade and placed in the broken glass receptacle.

**Table 2.2:** Fluidic Components for Devices

| Component | Vendor | Item Number |
|---|---|---|
| NanoTight™ PEEK for 1/16" OD | IDEX, Inc. | F-333N |
| FEP Tubing 1/16" OD | IDEX, Inc. | 1520L |
| Female LuerTight™ Fitting 1/16" OD | IDEX, Inc. | P-835 |
| Solvent Resistant Tape, 0.0039" thick | McMaster-Carr | HT6240 |
| Permanent Double Sided tape | 3M™ | 665 |
| Coverglass #1.5H D 263 M Schott Glass | Ibidi | 10812 |

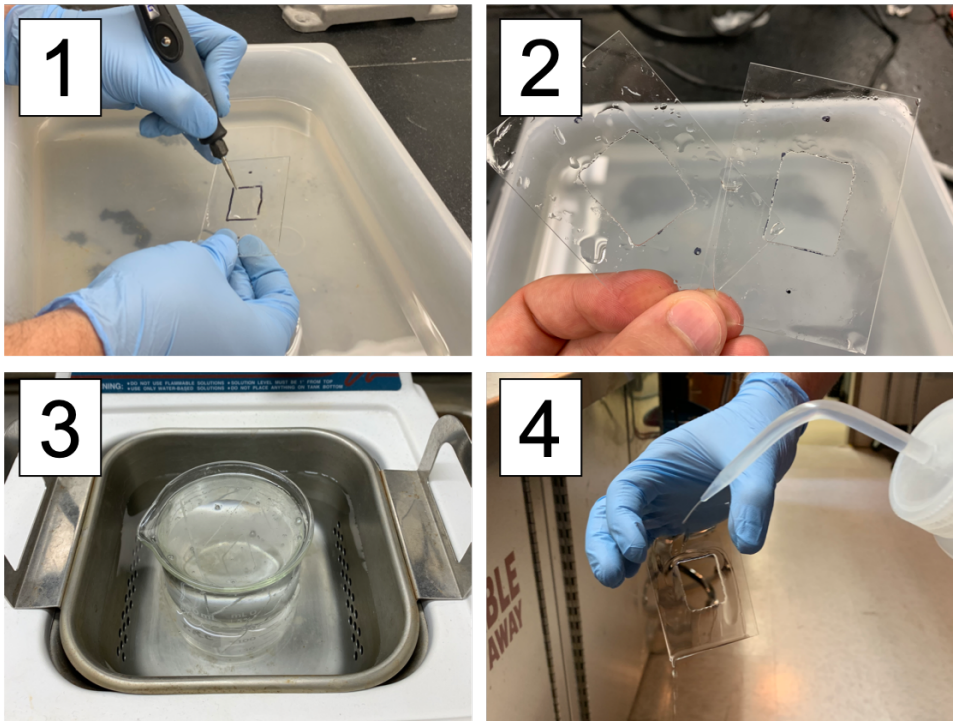


**Figure 2.3:** Procedure of the glass flow cell, steps 1-4

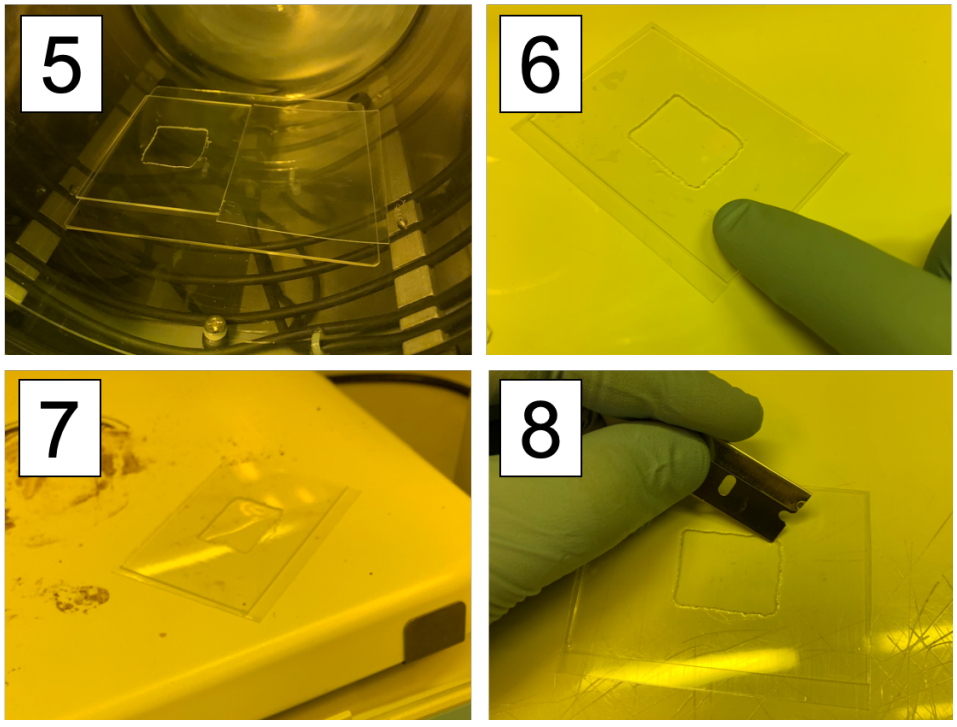


**Figure 2.4:** Procedure of the glass flow cell, steps 5-8

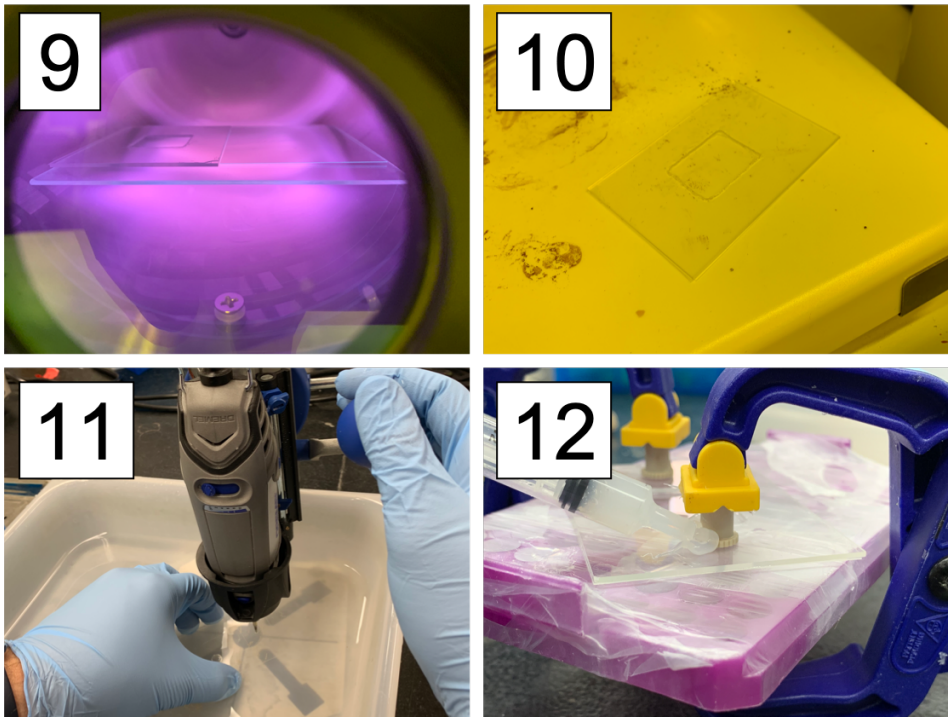


**Figure 2.5:** Procedure of the glass flow cell, steps 9-12

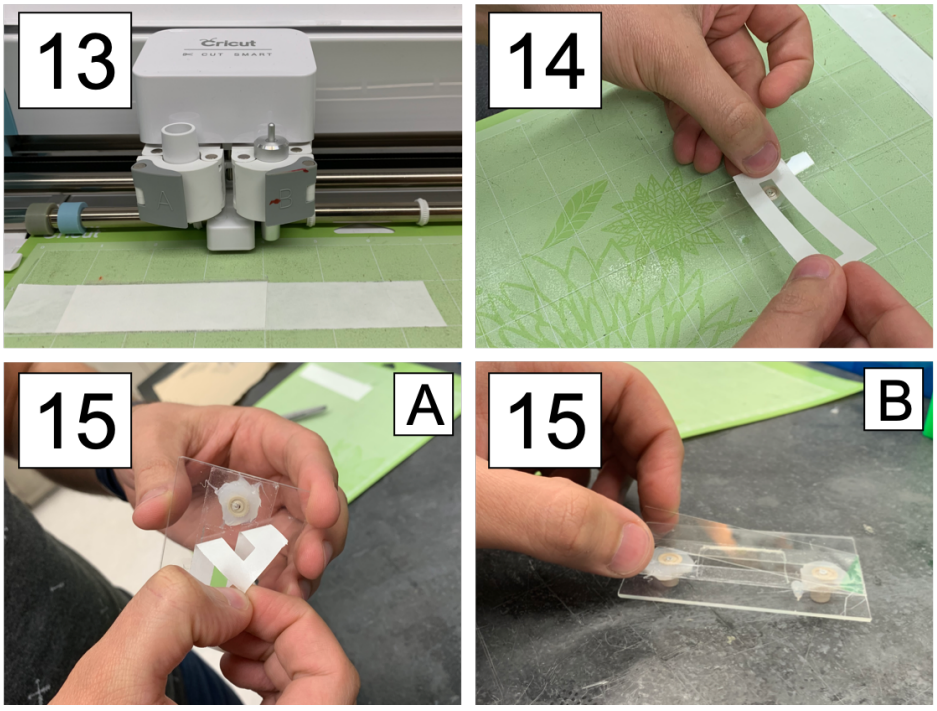


**Figure 2.6:** Procedure of the glass flow cell, steps 13-15

### 2.3.2 Permanent Flow Cells

The glass flow cell was beneficial at first, however, we realized that the glass flow cell succumbed to breakage. The glass flow cell would often break when removing the final coverslip that completed the flow channel. We removed the final coverslip from the glass base for a variety of reasons, the most important being our living system studies. We need to remove and disinfect the device from contact with the cells, and this is done by removing the glass and discarding in biohazardous waste. A second reason why we remove the final coverslip, is degradation of the solvent resistant tape used to adhere it to the glass base. While the tape is "solvent resistant" it is not fully solvent proof. This leads to the tape dissolving over time and the coverslip needing to be replaced due to the seal of the channel being compromised. When removing this glass coverslip, if not careful enough, it can cause a crack in the coverslip bonded to the glass base which compromises the whole flow cell. Because of this, we decided to come up with a more permanent option that would last longer and for multiple uses in the lab. This version added in a second layer of PDMS that had a laser-cut channel, instead of having to scrape and remove the second coverslip channel after each use. This permanent version was advantageous being that it only needed to be rinsed with solvent and nitrogen after use and could be used with a variety of solvents with no degradation to the PDMS channel. However, it is disadvantageous because there is no way to completely sterilize the channel or functionalize the glass coverslip to immobilize cells to the channel for living system studies. The second version of the permanent flow cell is a completely different concept in where the piece is machined out of a chemically and thermally resistant material, reusable, and will not break upon use. The details of each "permanent" model will be described in detail below.

#### Glass PDMS Permanent Flow Cell

As previously mentioned, this version of permanent flow cell is a modification of the glass flow cell in 2.3.1. This more permanent version contains a second bonding step where a laser cut layer of PDMS replaces the double-sided tape layer for the flow channel. It is bonded to a second coverglass instead of having to scrape and replace the second coverslip where

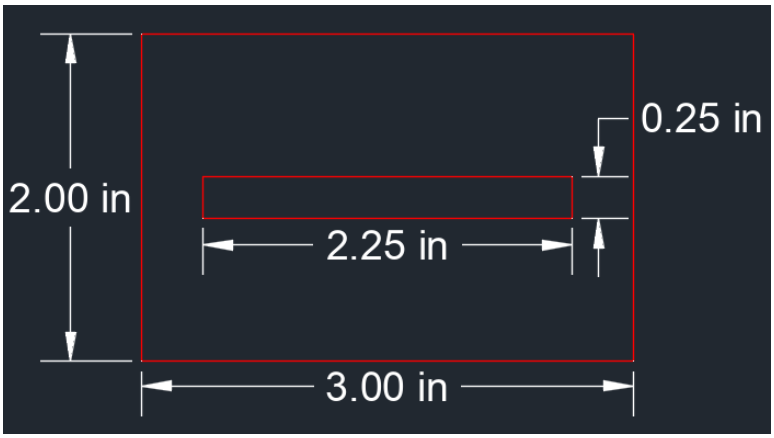


**Figure 2.7:** Laser Cut PDMS Layer

breakage issues were occurring previously. The laser cutter used was in Dr. Christopher Baker's lab in the UTK Chemistry Department. The outline of the cut used for this layer can be seen in Fig 2.7. Once bonded, the same ports used in the all-glass flow cell from IDEX, Inc., were placed and siliconed onto the large glass slide and dried overnight. Before use, the microfluidic tubing was screwed into the silicone ports and the flow cell was adhered to the microscope stage using 3M™ double-sided tape. After use, the PDMS "permanent" glass flow cell is simply cleared with nitrogen gas, rinsed with acetone, and then dried with nitrogen again for the next usage. Using this permanent glass flow cell with PDMS led to great success in the lab for flowing solutions. However as mentioned, these devices were not optimal for cell studies because they could not be completely sterilized. We also realized that breakage was becoming another issue with them, and because of the second layer of bonding and laser cutting, the process became time-consuming. Once these broke, due to the extra bonding and drilling needed, production time led to a couple of hours per device. This inspired us to create a design that was not reliant on glass and to move toward a less breakable material that was still thermal and chemically resistant which will be described below.

### Machined Permanent Flow Cell

After some preliminary research on materials and a consultation with our in-house machinists Timothy Free and Danny Hackworth, we came up with a design to machine a base for the

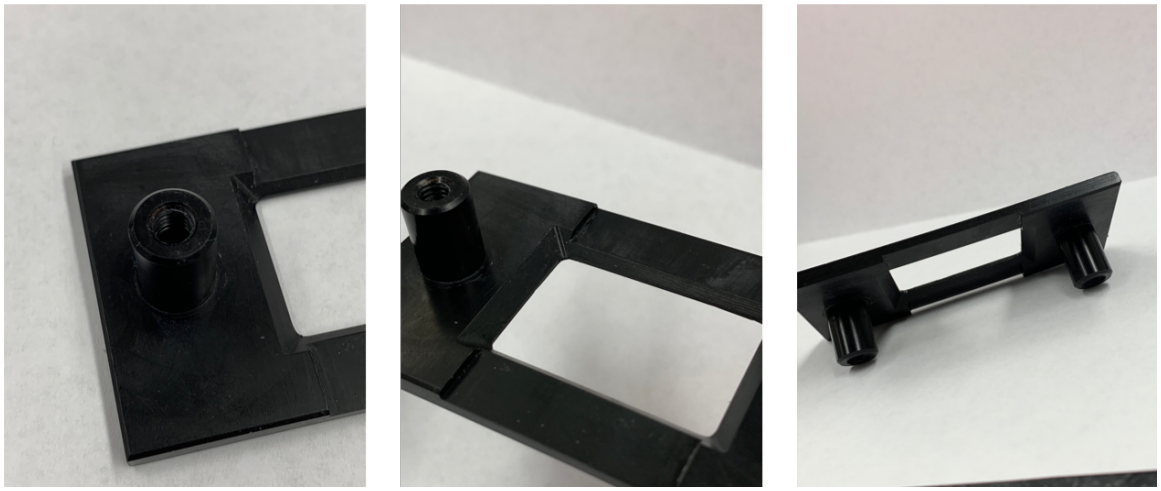

**Figure 2.8:** Machined Flow Cell out of Delrin® material

flow cell out of Delrin® material. This base is similar in size to a 25mm x 75mm glass slide, with some extra room for support. The edges are beveled to fit the collection objective, and the ports used from IDEX, Inc. that are normally siliconed onto the glass-based devices are no longer needed because the machined base is already built up and threaded as necessary to fit the screw-in tubing ports for flow. When ready to use the permanent flow cell, a 25mm x 75mm coverslip is adhered to the base with two strips of 3M™ double-sided tape. After this, the Dremel® is used to drill the holes needed to flow into this first coverslip. The flow cell is now dried with nitrogen and rinsed with acetone and ethanol to remove and excess glass dust residue from drilling. A Cricut® flow cell channel made out of the solvent resistant tape is now placed onto the coverglass and gentle pressure is applied to adhere the first part of the tape. The second layer is removed and a second piece of coverglass is placed onto the tape creating the flow channel. Gentle pressure is applied once again to form the channel and to ensure a tight seal. The flow cell is now ready for use, where the microfluidic tubing can be screwed directly into the built-in ports on the device. This flow cell is also adhered to the microscope stage with 3M™ double-sided tape. This base holds up well against a variety of solutions, solvents, and heat, and has been used for almost a year with no signs of degradation. The Delrin flow cell device can be seen in Fig 2.8. In the Delrin based permanent flow cell, all glass is removed after each use, which only takes a few seconds to do and ensures no left-over solution from a previous use, and also ensures and living cells are

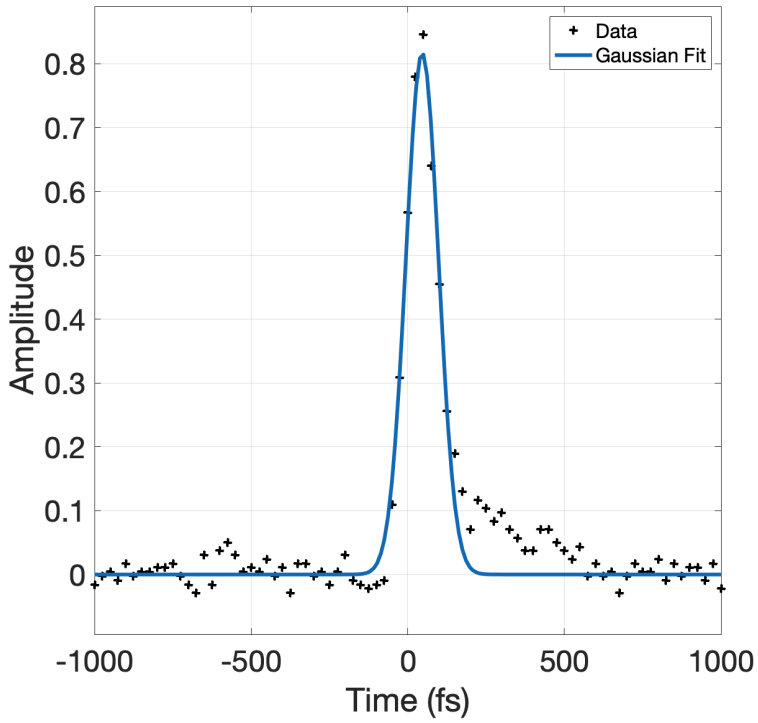


**Figure 2.9:** Pulse compression scan applied to a Gaussian fit resolving a FWHM of 73.5 fs

properly removed and disposed of. A razor blade is used to remove both glass layers from the base. To remove any residual adhesive, the device is placed in an acetone bath for a few minutes and the adhesive is gently scraped off again with the razor blade.

### 2.3.3 Pulse Compression

As mentioned previously, one reason for creating a more permanent flow cell device is for flowing carbon disulfide ($CS_2$) to optimize pulse compression and to get the instrument response. This solvent gives a non-resonant signal when pumped with 400 nm light and probed with 550 nm light.[55] This process only occurs when the pulses are overlapped temporally and spatially. However, $CS_2$ is known to have a strong odor and also rapidly evaporates. Previously, a small amount of $CS_2$ would be sandwiched between two glass coverslips and placed to use on the microscope to obtain our TAM measurements. However, because $CS_2$ evaporates rapidly, this method could not suffice for the time period required to run the genetic evolution program with the spatial light modulator (SLM) which we use to compress the light.

In the genetic evolution model, the TA intensity signal of $CS_2$ is run through a LabVIEW code. The code takes the signal output from the LIA and applies a phase to the SLM device, which will in-turn increase or decrease signal. The code "evolves," meaning once an increase in signal is found, it will go with these parameters and keep improving.[47, 65, 41, 48] This is ran for multiple generations until signal improvements start to increase and then stabilize.

With the permanent Delrin-based flow cell, the stability and robustness of the new device led to more replicable and stable scans for pulse compression, while lessening the negative side effects of the exposed solvent. Pulse compression is important for TAM studies, especially when studying the lifetimes of molecules. An instrument response is needed to properly fit the data to get out the exponential lifetime of the sample that was measured. An example of a pulse compression scan that gives the instrument response and how the data is fit can be seen in Fig 2.9. The data is fit to a Gaussian with one exponential and resulted in a full width at half maximum (FWHM) of 73.5 fs.

Many factors in the lab cannot be controlled, such as temperature and humidity, all which can affect the laser. Checking compression daily can lead to better knowledge of the collected data and better understanding of the results. The development of a more robust way to flow $CS_2$ over our microscope has led to a faster way to check compression each day before experiments are conducted.

### 2.3.4 Studying Ultrafast Dynamics

Along with using flow cells to aid in pulse compression, they are used to flow solutions for studying ultrafast dynamics with TAM. The flow cell allows for fresh solution to flow through the focal spot of the TAM system which helps minimize photobleaching to the sample.[52] The flow cells have been used to optimize the TAM system with IR-144 laser dye, while pumping with 800 nm light, and $\beta$-carotene, while pumping with 400 nm light as seen in Fig 2.10.[36] Here, the data was fit to a single exponential from Zewail, et al.[66] to resolve a lifetime of $\sim$9.5 ps. These solutions have been previously studied with TA, verifying that the instrument is operating correctly and efficiently.[42, 46]

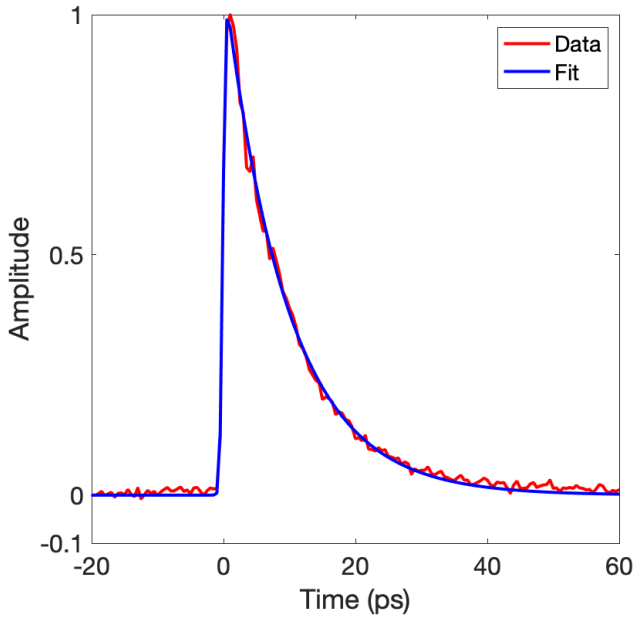


**Figure 2.10:** Data and fit of a TA scan of 500$\mu$M $\beta$-carotene in acetone. Fit to single exponential resolving a lifetime of ~9.5 ps.

Most importantly, the antifungal drug Amphotericin B (AmB) has been studied with TAM using these flow cell devices. More detail about the studies taken place with AmB will be discussed in Chapter 3.

### 2.3.5 Studying Drug-Membrane Interactions

The flow cells can also be used in the study of drug-membrane interactions in both living and model systems. Because of the thin channel in the device, model and living yeast cells can be immobilized onto the interior of the flow channel while introducing the drug through the port via a syringe pump for monitoring the interactions in real-time with TAM. The ability to introduce the drug while simultaneously monitoring the interactions on our TAM system was a great step in the progress of our AmB project. How this was done will be discussed in-detail in Chapter 3.

**Table 2.3:** Flow Cell Comparison

| Flow Cell Model | Advantage | Disadvantage |
|---|---|---|
| All Glass | • Allows for tight-focus with high-NA objectives<br>• Allows for use of cells in the flow channel | • Easily broken when cleaned<br>• Time-consuming to manufacture |
| PDMS Permanent | • Allows for tight-focus with high-NA objectives | • Easily broken when not handled carefully<br>• Does not allow for cell studies<br>• Can not be sterilized completely |
| Delrin Permanent | • Allows for tight-focus with high-NA objectives<br>• Allows for use of cells in the flow channel<br>• Efficient for removing and replacing glass<br>• No mess with silicone on ports | • Can not be made independently in the lab |

## 2.4 Conclusion

Flow cell devices have been shown to be beneficial to TAM in a variety of ways. Having this piece of equipment is crucial in the study of ultrafast dynamics of solutions, to probe excited states of molecules and study their lifetimes. They are also important in the study of drug-membrane interactions. The ability to introduce a drug to a living or model system slowly while observing the response of the system in this flow cell device was very beneficial to our lab. In this work, the new device that was developed led to overcoming the challenges that the all-glass devices had. The new Delrin based device overcame the challenges of background signals, breakage, and comes with reliability and a more robust and permanent design. Having this new design has led to greater productivity, more options for experiments, and better cleanliness in the lab. A comparison of the flow cells produced in our lab can be seen in Table 2.3. The opportunity to have a more robust design now opens the doors to many more studies that can take place with these devices.

# Chapter 3

# Transient absorption studies of Amphotericin B

## 3.1 Motivation

As mentioned previously in section 1.3, the mechanism of AmB has been debated significantly over the years.[24, 59, 3, 30, 49, 14] This lack of understanding of the mechanism limits a more targeted approach in the design of an improved version of the drug to lessen its severe side effects. Three models have been proposed in the literature with no actual conclusion on how the drug is causing cell death in fungi. Traditional optical microscopy studies of the drug by fluorescence are not possible, due to AmB having a low quantum yield ($\phi = 0.0006$).[31] The quantum yield, as shown in equation 3.1 of a molecule is defined by the number of photons emitted over the number of photons absorbed.

$$\phi = \frac{\#\text{ of photons emitted}}{\#\text{ of photons absorbed}} \tag{3.1}$$

A typical fluorescent molecule such as fluorescein, has a quantum yield of $\phi = 0.97$, demonstrates that AmB is *very* weakly fluorescent.[58] In AmB, the drug would require a bulky fluorescent probe that could possibly affect the natural interaction of AmB with fungi due to these probes being almost as large as the molecule itself.[53, 67] However, the polyene in AmB, gives us the ability to study the molecule label-free with transient

absorption microscopy (TAM). Due to this debate, the efforts in our lab have been aimed to resolve how AmB is interacting with living systems, and ultimately image the interaction *in vitro*.

## 3.2 Ultrafast Dynamics

To study the interaction of Amphotericin B with the membranes of both living and model systems, we first had to obtain a valid signal response from the drug with our TAM system. This started the study around a known carotenoid system, $\beta$-carotene. A carotenoid is a natural pigment found in fruits and vegetables that is characterized by a polyene backbone.[7] AmB also contains a polyene backbone similar to $\beta$-carotene, however, shorter in length. $\beta$-carotene has been studied previously with TAM using a 400 nm pump pulse followed by a 550 nm probe pulse, which has been shown to give intense signal due to its characteristic polyene backbone.[61] These wavelengths were selected for AmB, because it also contains a similar backbone as seen previously in Fig 1.5, just differing in length. In $\beta$-carotene, the absorption of blue-green light corresponds to the transition from the ground state ($S_0$) to the second singlet excited state ($S_2$). Due to molecule symmetry, the transition from the $S_0$ to the first excited state ($S_1$) is not possible.[42] When in the $S_2$ state, the molecule rapidly relaxes to the lower excited state ($S_1$) by internal conversion and populates the $S_1$ state within $\sim$195 femtoseconds.[38] From here, the $S_1$ state now relaxes to the $S_0$ ground state on a slower picosecond timescale, $\sim$10 ps. We have seen AmB participate in similar, however slower, excited state dynamics than $\beta$-carotene. This has also been cited in the literature but not extensively proven.[31, 32] Our AmB studies started by following previous work as mentioned above on $\beta$-carotene. We obtained signal using our TA system with a 400 nm pump pulse and a 550 nm probe pulse, following the same conditions for $\beta$-carotene and can be seen in Fig 3.1. The fitting of the data is also shown in Fig 3.1 and was fit to a single exponential from Zewail, et al.[66] to resolve a lifetime of approx. 300 ps which corresponds with previous fluorescence lifetime studies of the drug.[32] The experimental conditions tested have been described previously, which consist of a 400 nm pump pulse and

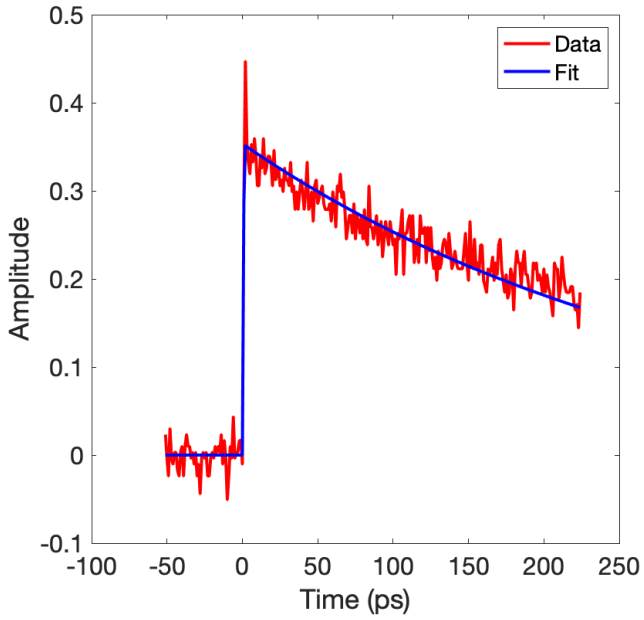


**Figure 3.1:** TA scan of 100 $\mu$M Amphotericin B in DMSO. Fit to a single exponential resolving a lifetime of ~300 ps

a 550 nm probe pulse.[35] We have studied various concentrations of AmB previously as low as 25 $\mu$M with these conditions.

## 3.3 Imaging the drug-membrane interaction on living systems

After understanding how AmB interacts with the TAM system, its interactions with living systems was investigated. These studies aimed to gain a better understanding of how the drug interacts with living systems, more specifically, the fungus *Saccharomyces cerevisiae*. *S. cerevisiae* was chosen as it is one of the most-studied experimental organisms.[12, 39]

### 3.3.1 Previous studies

In the studies performed by Kevin Higgins, a previous graduate student in the lab, results showed clusters appearing after incubating AmB with *S. cerevisiae* as shown in Fig 3.2.[35] In this study, the cells were immobilized onto the coverslip with a 1:1 solution of 2 mg/mL

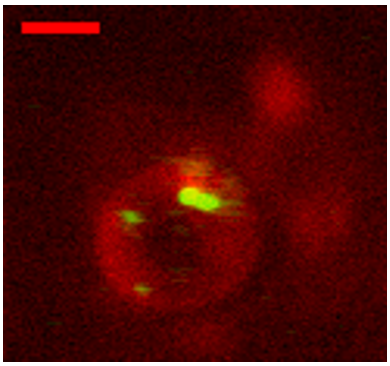

**Figure 3.2:** TAM image of the *S. cerevisiae* cell in YPD media interacting with 50 $\mu$M AmB taken 90 minutes after drug was introduced. Red signal is autofluorescence and green signal is arising from TA. Scale bar is 2$\mu$m. From ref. [35]

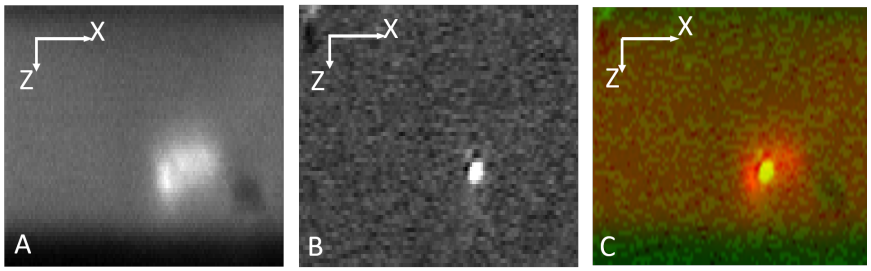


**Figure 3.3:** X-Z TAM images of 250$\mu$M AmB interacting with an *S. cerevisiae* cell. (A) Autofluorescence image locating the cell, (B) TAM image to locate the AmB appearing as a bright dot , (C) overlay of the two images to show where the AmB is located within the cell. All scale bars are 2 $\mu$m. From ref. [35]

concanavalin A (ConA) and 0.1% poly-l-lysine solution. The cells were "sandwiched" between to pieces of coverglass and placed onto the microscope. This was then attempted to be verified with a z-type scan on a piezo stage in Fig 3.3. Here, the cells were immobilized to the bottom coverslip of a flow cell and YPD media and AmB are flowing over the cells. The outline of the cell in Fig 3.3 A is not clearly defined, however, it can be seen that the AmB is shown as a bright cluster, but without the full 3D scan the location can not be confirmed. These were interesting results because this possibly demonstrated clusters of AmB internalizing into the cells. The previous studies all yielded the same results demonstrating clusters of AmB present.

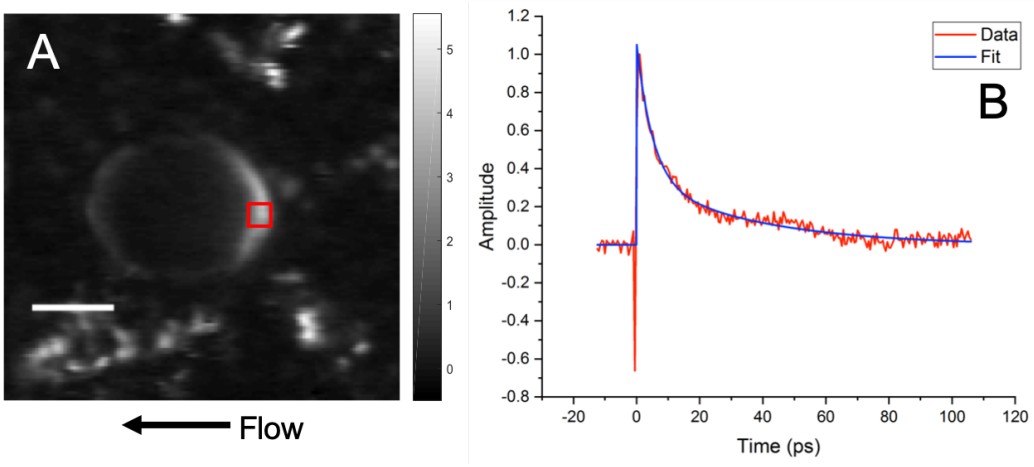


**Figure 3.4:** [A] *S. cerevisiae* cell with 250$\mu$M AmB/YPD solution flowing over in glass flow cell device. Scale bar is 2$\mu$m. [B] TA time-trace scan of the red boxed area on [A] TA data is fit to a double exponential resulting in a shorter lifetime component of 5.1 ps and a longer component of ~37 ps.

### 3.3.2 Recent studies

The imaging studies of AmB were revisited recently due to the unconfirmed explanation of the clusters and the inability to consistently reproduce the results seen previously. The previous results were obtained with unpolarized light into the microscope, and were rare to obtain. If they were obtained, the clusters would appear. If no signal was present for that experiment, there was no results. The recent studies included using the flow cell devices to introduce the drug over time. Initial flow cell studies with *S. cerevisiae* and AmB produced interesting results. As shown above in Fig 3.4A, there is a rise of signal to the right of the cell, shown in a smooth formation possibly suggesting a membrane accumulation. The TA scan shown in Fig 3.4B verifies a TAM signal giving a lifetime from this "lighted-up" area, possibly demonstrating AmB. This data was fit to a second exponential from Zewail, et al.[66] and resolved a shorter lifetime component of 5.1 ps and a longer component of ~37 ps. While this lifetime does not directly correspond to AmB, since the drug was in a water-based cell media and was aggregated, the aggregated lifetimes may tend to be shorter than previously seen in monomeric solution. This is also shown later in section 4.3 where the data in Fig 4.4 was also fit to a similar lifetime and is known to be aggregated in solution. When looking at this data, it is also important to note that this accumulation was

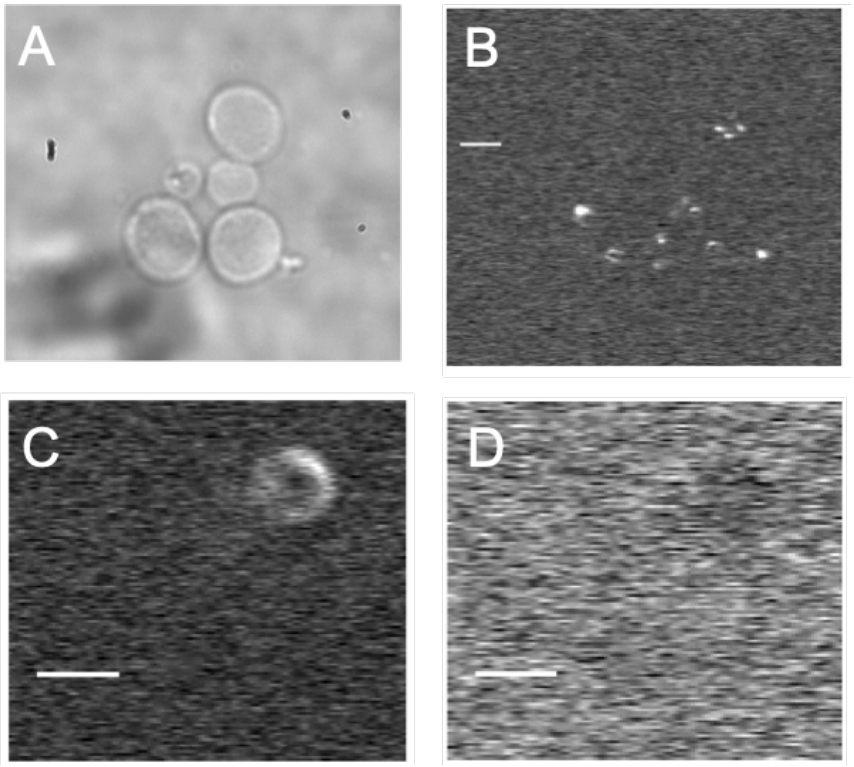


**Figure 3.5:** (A) Brightfield image of S. cerevisiae of image (B). (B) TAM image of the cells interacting with 250 $\mu$M AmB after 30-minute incubation, scale bar is 2 $\mu$m. Cells grown in LFM and immobilized with poly-l-lysine and ConA mixture. (C) TAM image of cells interacting with 250 $\mu$M AmB after 30-minute incubation, scale bar is 2 $\mu$m. Cells grown in LFM and immobilized with ConA only. (D) Same location as (C), but time delay set to a time delay before signal. Bright spots in the TAM images (B, C) are TA signal spots arising from the AmB.

also seen in the direction of flow in the flow cell chamber. It can not be concluded that the accumulation was actually interacting with the membrane or accumulating simply due to the flow of drug in this direction. Along with flow cell studies, other parameters such as media choice and immobilization method were changed to further study the drug. With these new parameters, different results were seen from the previous studies mentioned in section 3.3.1. Media was changed due to an abundance of background fluorescence given in yeast-peptone-dextrose (YPD) media when imaging cells with the TAM system. To combat this issue, a low fluorescent media (LFM) was used which gives less background fluorescence. The LFM is made in-house from a readily available protocol from the University of Wisconsin-Madison and *S. cerevisiae* has been shown to grow comparatively to YPD media.[44]

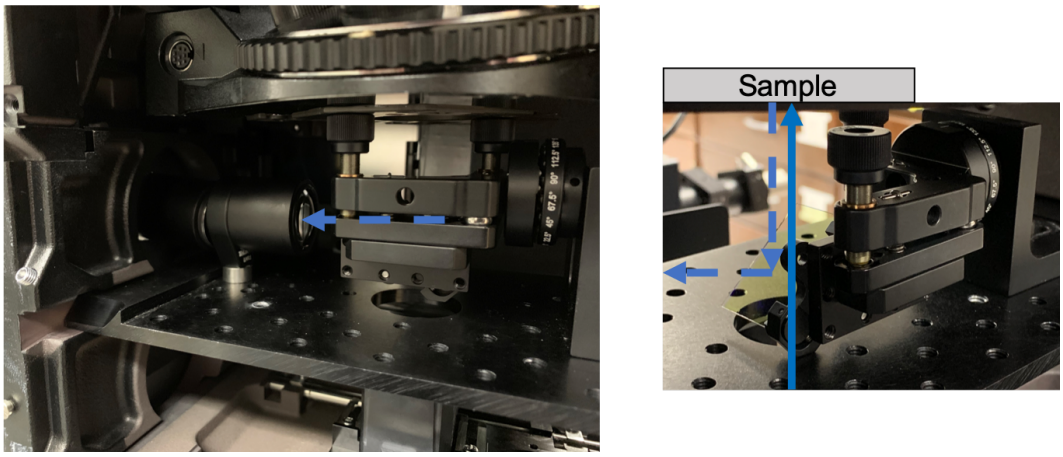


**Figure 3.6:** Image of the autofluorescence setup on the TAM microscope under the excitation objective. On the left, the 40 mm lens which focuses onto the fiber can be seen. On the right, the magnetic mount that holds the 472 nm dichroic that reflects the autofluorescence to the PMT. The solid blue line represents the 400 nm light and the dashed blue line represents the reflected autofluorescence

Using the flow method, we experienced AmB crashing out of solution over time when flowing over the cells. Due to the issue in inconsistencies with the flow on the cells and the instability of the AmB solution, the "sandwiching" method was revisited. In this recent study shown in Fig 3.5, the cells were grown in LFM media at 30°C overnight and diluted to 0.05 $OD_{600}$ and let grow to the log phase at 0.2 $OD_{600}$. Cells were then immobilized with a 0.1% poly-l-lysine:ConA solution. The bright spots in Fig 3.5B are from AmB signal. Here, we see clusters as shown previously, but can not conclude whether AmB may be aggregating and/or inserting itself into the membrane of *S. cerevisiae* in Fig 3.5B. However, when compared to Fig 3.5A, which is a brightfield image, the bright spots in Fig 3.5B may correlate to the membrane. When the same LFM media is used with only ConA immobilization method, different results can be seen. In Fig 3.5C, instead of clusters a membrane-like circular shape can be seen, this can possibly correlate with one of the membrane models mentioned previously. The bright spots are confirmed to be TA signal of AmB by changing the time delay to before pulse overlap and noticing that these bright signal spots disappear in Fig 3.5D. From these new studies, results differ from the previous data shown in section 3.3.1. This may be due to a change in media, or the immobilization method. Ultimately, at this point,

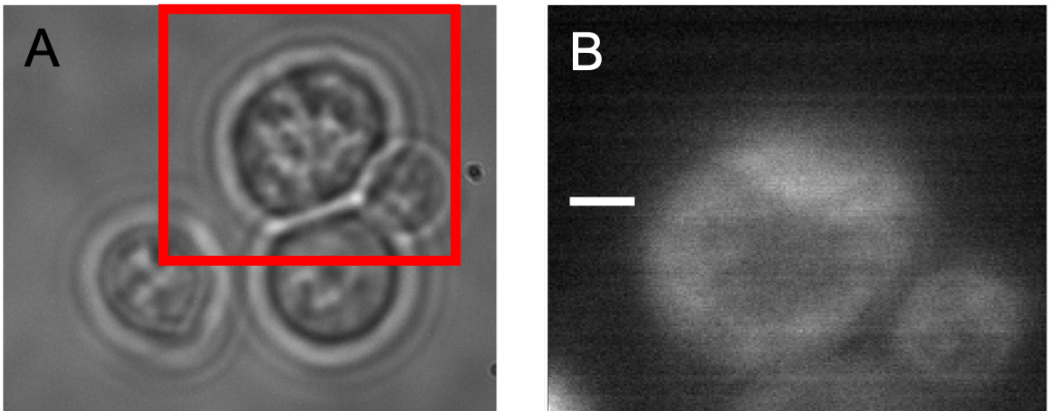


**Figure 3.7:** [A] Brightfield image of *S. cerevisiae* cell [B] Autofluorescence image of *S. cerevisiae* cell of the red boxed area on [A], scale bar is 2$\mu$m

we can not conclude where AmB is interacting with *S. cerevisiae* and further investigations with more control studies need to take place.

When these studies were not conclusive, the autofluorescence capabilities were modified back into the TAM system for future studies. This autofluorescence setup is different than the previous version, due to the ability to maintain polarization and the ability to easily collect autofluorescence and TAM data simultaneously. The previous autofluorescence setup was collected below the laser input to the microscope and was simply collected with a silver mirror onto the PMT. This new setup results in a cleaner signal by only reflecting the desired wavelengths, and also has the ability to remove and install the optics whenever needed since the dichroic mirror is placed on a magnetic mount. Since *S. cerevisiae* naturally autofluoresce, building this back in to the system will help to confirm some of the future data. In collection of the autofluorescence data, the 550 nm probe beam is blocked to the sample, and the 400 nm pump beam is allowed to reach the cells. A 473 nm band-pass dichroic mirror is placed below the excitation objective to allow for the 400 nm light to pass through and the 472 nm autofluorescence of *S. cerevisiae* to be reflected to a photon-counting photomultiplier tube (PMT). The signal is reflected onto a 40 mm lens and focused onto a fiber which is then coupled into a lens tube on the PMT where it is "cleaned up" with a 472/30 band-pass filter and focused onto the PMT detector with a 35mm lens. Alignment of the PMT was completed with TetraSpeck™ beads to achieve the highest photon count. After alignment of the PMT, *S. cerevisiae* were grown and immobilized onto a glass coverslip

with ConA solution only. A second glass coverslip was placed over and "sandwiched" on the cells and sealed with Valap. The cells were placed onto the microscope and observed with the excitation objective only. The setup can be seen in Fig 3.6, where on the left, the lens is shown and the dashed arrow represents the autofluorescence signal that would be getting sent from *S. cerevisiae*. On the right of Fig 3.6 the dichroic mirror can be seen, where the 400 nm light is allowed to pass through and the 473 nm autofluorescence is allowed to be reflected to the PMT. It is also shown that the dichroic is placed on a magnetic mount and allows for precision alignment. The results from using this new setup can be seen in Fig 3.7. In Fig 3.7, the red outline is then enlarged to the left. Here, the autofluorescence of *S. cerevisiae* is shown being excited by the 400 nm pump pulse only. Building the autofluorescence setup back into the TAM is a great step forward into confirming some of the AmB studies, however as we modified our system conditions as to be discussed in chapter 4.3.2 this was not able to be done. However, now that the method to collect autofluorescence followed by a TAM image is now in place, future studies are now setup to be more confirmatory.

## 3.4 Imaging the drug-membrane interaction on model-membrane systems

Along with the living system studies, we also moved forward with studying the interaction of AmB on model systems. Imaging AmB interacting with model membrane systems will lead to further discovery of the drug and its mechanism independent of environmental factors and free from cellular components. Using model membranes, we can also alter the lipid composition along with the sterol content more easily than in the living system. Model membrane systems come in various sizes, including small unilamellar vesicles (SUVs), large unilamellar vesicles (LUVs), and giant unilamellar vesicles (GUVs) which are tens of microns large.[17, 18] For our studies, we used GUVs (1-10$\mu$m) which are closest in size to *S. cerevisiae* which is approx. 5 $\mu$m in size.

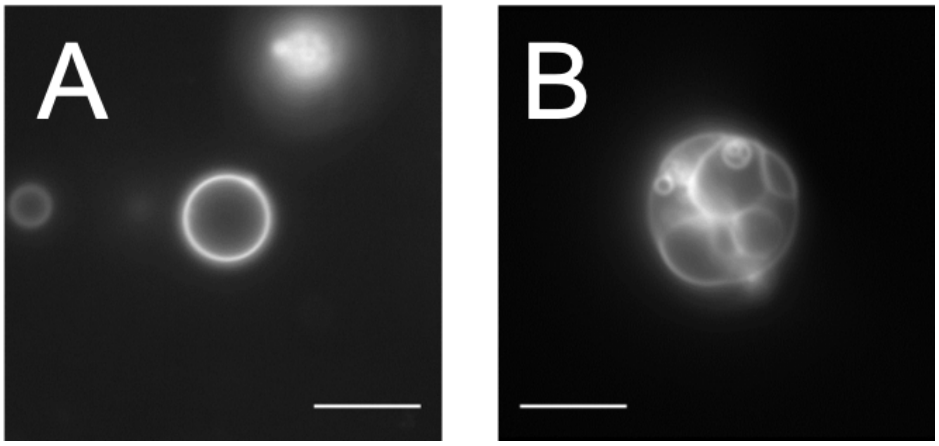


**Figure 3.8:** [A] Image of POPC-only GUV stained with FM4-64 [B] MVV with POPC-only and incorporated with 5% biotin stained with FM4-64 dye. All scale bars are 5 $\mu$m

### 3.4.1 Preparation of vesicles

Preparing the model membrane system can be completed in one of two ways: gentle hydration or electroswelling by a device. Both methods have been experimented with in the lab. Gentle hydration involved many complex steps and led to inconsistent GUVs that were not stable over long periods of time. Because of this, a commercial device called the Vesicle Prep Pro by Nanion Technologies was used that has been proven to be reliable in the literature.[13] It allows for formation of GUVs from 1-30 $\mu$m in diameter. To form the ideal GUV, parameters such as temperature, current amplitude, and frequency can be manipulated to customize the final GUV product.

We can also vary the lipid composition and introduce other components such as sterols into the membrane as needed to mimic the conditions of a living system. Only GUVs containing 1-palmitoyl-2-oleoylphosphatidylcholine (POPC) have been synthesized so far and were produced to model *S. cerevisiae*. The conditions used consisted of 3V and 10 Hz for 120 minutes. This produced GUVs with a size of $\sim$5 $\mu$m, which was desirable due to *S. cerevisiae* being approx. 5 $\mu$m in diameter as well. The GUVs were observed using the fluorescent dye, FM4-64. The fluorescent dye was in solution with DMSO and was incubated with the GUV solution for approximately 30 minutes before imaging on the microscope. Results from the Nanion device can be seen in Fig 3.8.

### 3.4.2 Studies on vesicles

Modeling the *S. cerevisiae* system with the model membranes for observing AmB's mechanisms was not able to be carried out in full due to time constraints. More of this study was spent on optimization of the GUV synthesis using the Vesicle Prep Pro device so a more robust and reproducible preparation method could be perfected for future use. The start of the GUV preparation using the Vesicle Prep Pro was to follow the base settings on the device along with a protocol provided in the manual. This called for a 10 mM POPC-only solution which was added in conjunction with a 0.2 M sucrose electroformation solution. Using the base protocol led to GUVs in the 5-10$\mu$m size range, however, many did not swell up very well and there were plenty of multivesicular vesicles (MVV) present in solution as shown in Fig 3.8[B]. Multivesicular vesicles are intrusive to our studies because these contain vesicles inside of vesicles, which is not desirable for studying drug-membrane effects. Due to this problem, the formation method was modified a few ways. The first was to increase the voltage from the base protocol to 3V and 10 Hz which produced consistently sized GUVs, however we attempted to increase the yield by changing the settings again to 4V and 10 Hz. However, this led to the same issues of unstable formation where we then settled at 3V and 10 Hz as the best formation setting due to the consistency of 5-10$\mu$m GUVs and the lack of MVVs present in the solution.

## 3.5 Conclusion

The studies that have been completed previously and discussed in chapter 3.3.1 and the recent studies discussed in chapter 3.3.2 show very significant differences in the data observed. The previous studies consistently showed internal clusters of AmB in scans. The recent studies also showed these clusters, but when environmental conditions were changed, ring formations appear. More control studies are needed to determine if the effects we are seeing are coming from the drug or from the environment. These controls include cells and only DMSO solution with no AmB, along cells and only the various immobilization methods. The addition of a new autofluorescence setup into the system will aid in future studies as a better way to confirm the cell location and where the drug may be interacting. The efforts discussed here

are not the end of the studies to be completed. The elucidation of the mechanism of action of Amphotericin B is still of utmost importance. Model membrane systems may be the start for understanding how the drug is interacting to different environments, lipid conditions, and sterol contents as they can be modified easily in the lab. Once these modifications are studied, and an idea of how AmB interacts with the changes in membrane compositions, living system studies should then be commenced with a focus on more control studies, an inclusion of autofluorescence, along with proper x-,y-,z-, scanning.

# Chapter 4

# The study of Fungizone®

## 4.1 Motivation

We can successfully obtain signal off of Amphotericin B with our TAM system and have been able to image interactions with the drug in living systems as shown in chapter 3. However, while these studies are still innovative and unique, the concentrations and the solvents being used in these studies are not at biologically relevant levels. In our previous study, AmB was used in a solution of dimethyl sulfoxide (DMSO) because of its low solubility in water. DMSO is a solvent with potential health hazards, and treatment with a solution made with this type of solvent would not be ideal.[26] Therefore, we have decided to look into a more commercialized solution used to treat life-threatening infections. Another reason why we decided to look into this solution, is its water solubility. In cell media, we have also previously seen AmB to fall out of solution over time due to its low water solubility. The commercialized solution is more commonly known as Fungizone® or "commercial AmB" and consists of AmB, sodium deoxycholate, and water. The sodium deoxycholate is used as a detergent to keep the AmB in suspension due to its low water solubility.[27] There are other formulations of AmB that exist as discussed previously in Chapter 1.3, however, the Fungizone formulation is the most readily available. After the interesting results seen in section 3.3.2 with the varying effects of immobilization method and media choice, we then shifted our studies to move toward studying Fungizone interactions with *S. cerevisiae*. The

main reason we moved to Fungizone was to continue our flow cell studies, while not having the additional concern of the AmB falling out of solution.

## 4.2 Preparation of Fungizone ®

The solutions that are available on the market are supplied in very low concentration ranges (250 $\mu$g/mL) which is approximately 270 $\mu$M. To first verify if the Fungizone would respond to our TAM system, the concentration of the AmB in the solution had to be increased severalfold to increase the ability to obtain signal on the solution, which can then be diluted further once the proper experimental conditions have been established. To do this, we formulated a solution identical to the Fungizone solution which contained a higher amount of AmB with the same molar ratio of sodium deoxycholate. The procedure was adapted from Gangadhar et al. to create a solution with 500 $\mu$M of AmB, double the concentration in the commercially available Fungizone.[27]

**Procedure**

1. 0.02073 g of deoxycholic acid sodium salt was added to 20 mL of ultrapure deionized water in a 50mL beaker and placed on a stir plate until dissolved

2. 0.0231 g of amphotericin B was added slowly to the mixture of sodium deoxycholate and water while maintaining constant stirring

3. 0.2 M sodium hydroxide solution was added dropwise with continuous stirring until solution turned clear

4. pH of solution was tested and adjusted with 0.2 M phosphoric acid until reaching a pH of 7.4

5. After a pH of 7.4 was reached and stabilized, the solution was brought up to a final volume of 50 mL and placed in the freezer after use

This solution was verified by UV-Visible spectroscopy and is shown in Fig 4.1 to match the commercial and homemade Fungizone, which also compares well with literature.[1, 27] The

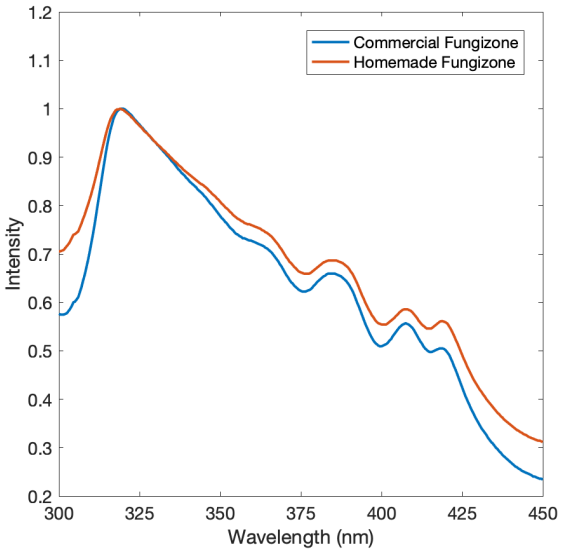


**Figure 4.1:** UV-Vis spectra of Commercial and Homemade Fungizone

homemade solution was also subjected to measurement by dynamic light scattering (DLS) to determine the size of the micelle-like particles formed. A Zetasizer instrument by Malvern Instruments was used in Dr. Bin Zhao's lab in the chemistry department here at UTK to determine the particle size of our solutions. The samples were ran in triplicate, and the z-average was found to be 46.27 nm for the homemade solution as shown in Fig 4.2, compared to a z-average of 53.90 nm in the Fungizone as shown in Fig 4.3. The results do not differ significantly meaning the solutions are still very similar in composition. Having the higher concentration of AmB present, will enable a greater probability of finding signal present with our TAM system. The solution can also be scaled up to increase the concentration of the drug if needed as long as the mole ratio of sodium deoxycholate and AmB remains consistent.

| | | Size (d.nm): | % Intensity: | St Dev (d.nm): |
|---|---|---|---|---|
| Z-Average (d.nm): 46.27 | Peak 1: | 60.60 | 93.3 | 34.56 |
| PdI: 0.365 | Peak 2: | 3099 | 6.7 | 1319 |
| Intercept: 0.931 | Peak 3: | 0.000 | 0.0 | 0.000 |
| Result quality : Good | | | | |

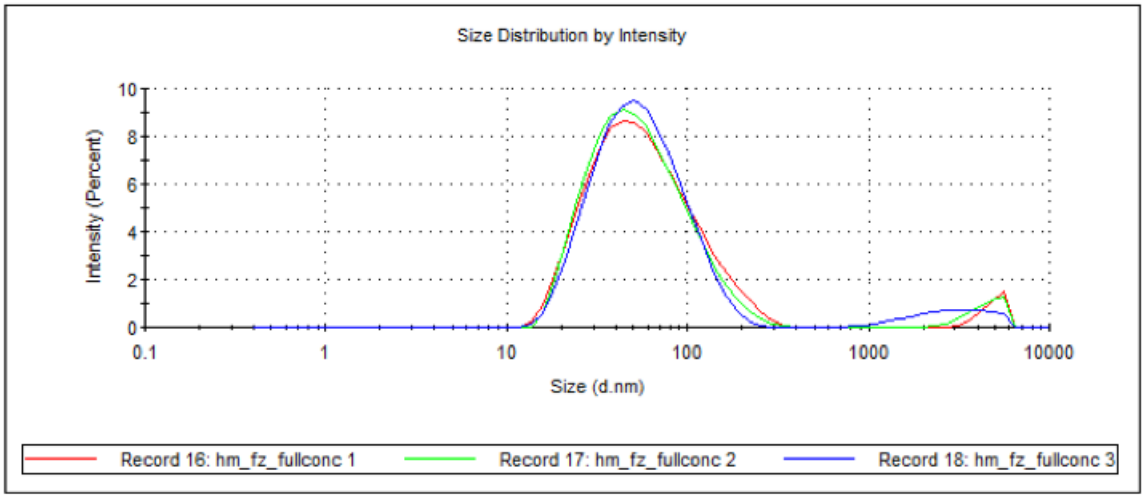


**Figure 4.2:** DLS measurement of homemade Fungizone

| | | Size (d.nm): | % Intensity: | St Dev (d.nm): |
|---|---|---|---|---|
| Z-Average (d.nm): 53.90 | Peak 1: | 82.18 | 100.0 | 54.96 |
| PdI: 0.285 | Peak 2: | 0.000 | 0.0 | 0.000 |
| Intercept: 0.934 | Peak 3: | 0.000 | 0.0 | 0.000 |
| Result quality : Good | | | | |

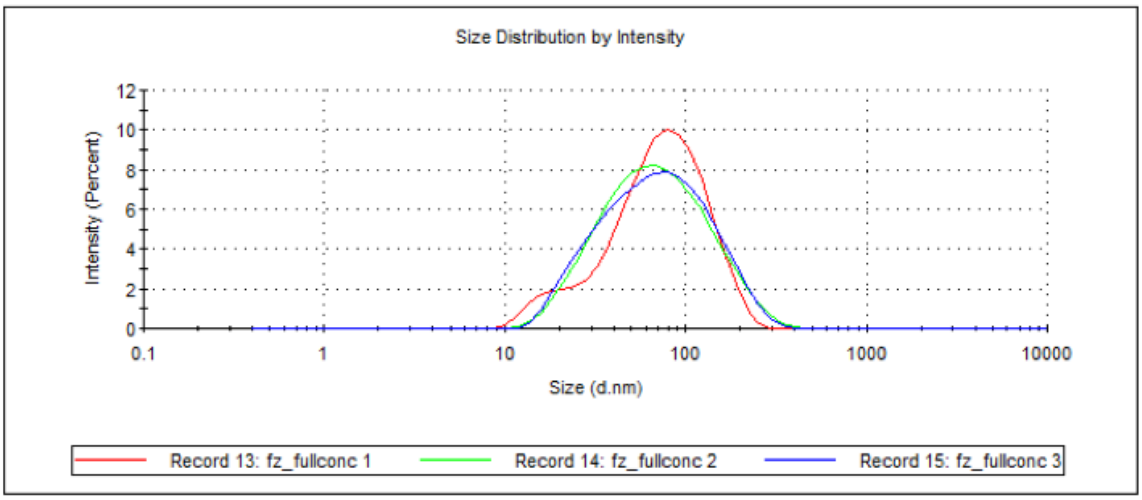


**Figure 4.3:** DLS measurement of commercial Fungizone

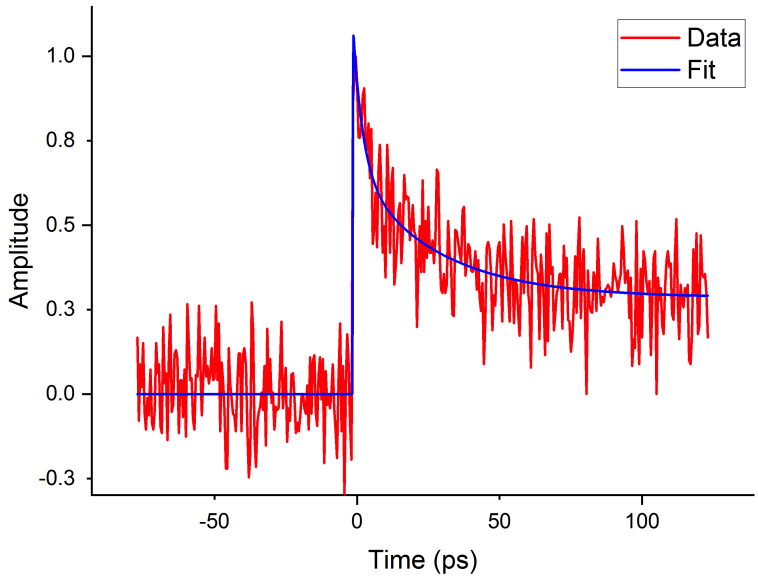


**Figure 4.4:** TA scan and fit of the 500 $\mu$M house-made Fungizone solution described in Chapter 4.2. Data is fit to a double exponential function resulting in a shorter lifetime component of 3.5 ps and a longer component of 29 ps.

## 4.3 Study of Fungizone® with TAM

### 4.3.1 Amphotericin B Conditions

Once a higher concentration of AmB was able to be formulated in the Fungizone type solution, it was placed into the Delrin flow cell device mentioned previously in Chapter 2. While AmB in DMSO is Amphotericin B in its monomeric state, the Fungizone solution is "controlled aggregation" meaning the drug is aggregated but still clear in solution. We expect this "controlled aggregation" to give different dynamics on solution, however, we first attempted to apply the same conditions that were used to the study monomeric Amphotericin B. A 400 nm pump pulse was used, followed by a 550 nm probe pulse. At first, results were expected to differ due to the aggregation present in the solution. However, we were surprised to see a small signal increase from baseline when testing this solution with the standard AmB wavelengths. While the Fungizone solution responded to the same experimental conditions it did appear that the dynamics shown are different than from monomeric AmB (solution in DMSO).

This small signal can be seen in Fig 4.4. While this small signal was exciting because we could get some of a response from the solution, it is not enough of an increase from the baseline for our imaging studies. This data was fit to a double exponential by Zewail, et al.[66] and resulted in a shorter lifetime component of 3.5 ps and a longer component of 29 ps. A 1 mM solution of Fungizone was also formulated in the lab and resulted in a similar response. This ultimately led to changing the experimental conditions in the TAM setup to get a better signal response which will be described in Chapter 4.3.2.

### 4.3.2 Modified Conditions

Due to the lack of response with the previous conditions used with Fungizone solution, we decided to change the experimental conditions on the TAM system. To start, we discussed our results with a colleague at Oak Ridge National Laboratory (ORNL), Dr. Yingzhong Ma. We provided Dr. Ma with a sample of Fungizone solution, and signal was obtained with the TA system at the ORNL lab. The TA setup there has the ability to scan over probe wavelengths and see which one would be optimal for a study. While ours has this capability as well, the white-light source at ORNL has higher stability and can produce better power for the probe source than our PCF device in the lab.

From the data shown in Fig 4.5[A], it can be seen that below 580 nm there is weak signal, and at approximately 635 nm, the highest signal can be seen from the solution. Due to the results obtained at ORNL, we have decided to therefore change our TAM setup in the lab to match the redder probe wavelengths to see this signal increase. It is important to note that Dr. Ma was pumping the samples at 360 nm instead of 400 nm. Dr. Ma was pumping at 360 nm to pump the aggregate peak as shown in Fig 4.5[B]. The aggregate peak of AmB can most clearly be seen at 325 nm and rises as aggregation increases, however, the peak at 360 nm also changes due to aggregation. Due to system limitations, we are pumping at the static peak centered around 400 nm. We expect to still see signal at this peak because this is present in all forms of AmB whether aggregated or monomeric, however, they may not show as intense as he has seen in his study. To do this, the first step is to probe the sample with a redder wavelength, and to switch the Femtowhite 800 PCF fiber which was used previously, with a PCF device that will provide more intense wavelengths on the redder

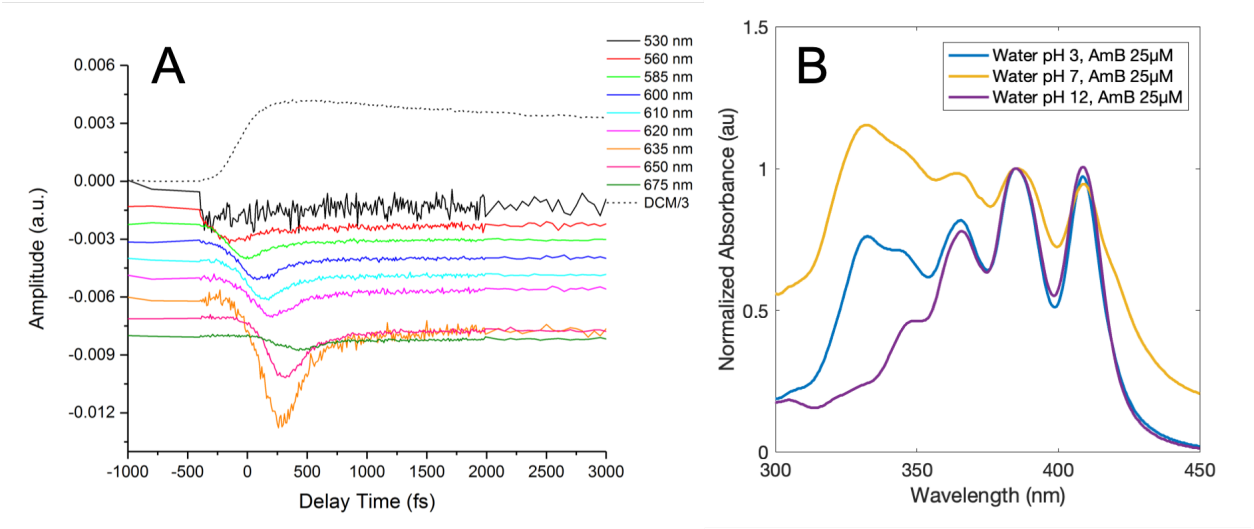


**Figure 4.5:** [A] TA scan from Dr. Ma at Oak Ridge National Laboratory of the Fungizone solution described in Chapter 4.2 [B] UV-vis spectra of 25 $\mu$M AmB in water at varying pH (adjusted with HCl or NaOH)

end of the spectrum. The Femotwhite CARS (coherent anti-stokes raman scattering) device provides a redder spectrum (>600 nm) as compared to the Femtowhite 800 as can be seen in Fig 4.6. While in this figure red wavelengths can be seen with the Femtowhite, these wavelengths are low in power and are not sufficient for our studies. The red wavelengths are extremely unstable, and the only stable wavelength for use in the Femtowhite 800 is the dispersive wave described previously in section 1.2.1. However, the CARS fiber is designed for intense redder shifted wavelengths as demonstrated in Fig 4.6. This fiber device will now allow us to probe our sample on with red-shifted wavelengths and can be tuned similar to the Femtowhite as discussed previously in Chapter 1.2.

Before the Fungizone solutions could be tested with the different fiber installed in the TAM system, other conditions had to be re-aligned and re-verified now that a change was made. Re-alignment with a new fiber in the setup required a change in the off-axis parabolic mirror directly after the fiber to re-collimate the light, and then an adjustment on the SLM line. The SLM line was to be adjusted due to the fact that a redder end of the spectrum was now being used in the system, and it was initially optimized for green-blue light. The first step when installing a new fiber device into the system requires a method called cross-correlation frequency-resolved optical gating (xFROG). xFROG uses both the 800 nm pump

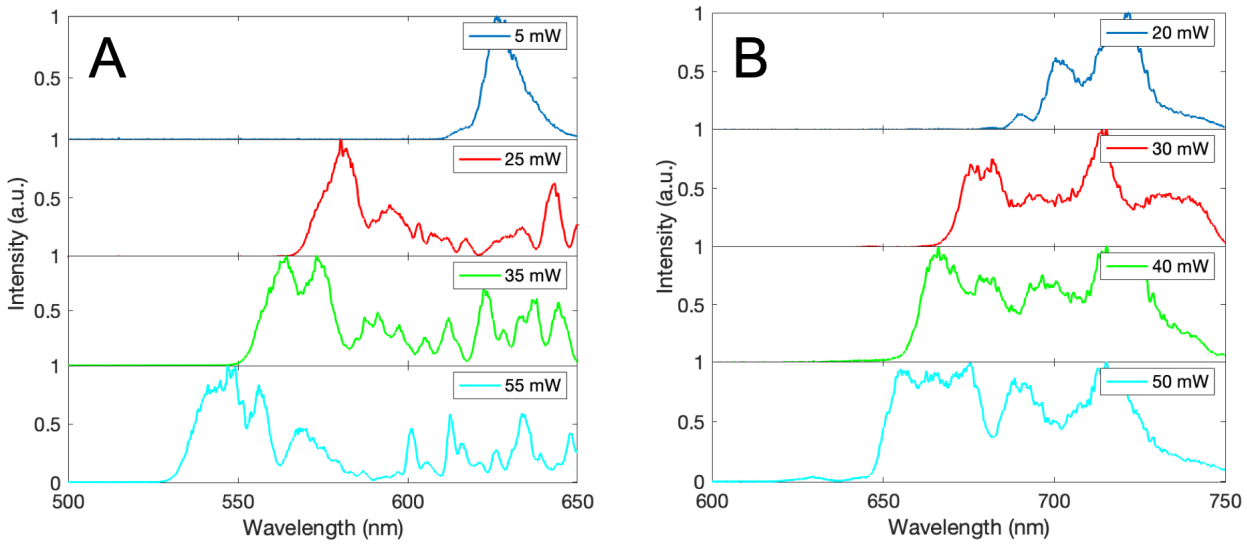


**Figure 4.6:** [A] Spectra of Femtowhite 800 PCF at varying 800 nm input power [B] Spectra of Femtowhite CARS PCF at varying 800 nm input power. Note the different wavelength ranges.

and the ∼600 nm probe pulses of light which become mixed in a non-linear crystal such as potassium diphosphate (KDP) to a create sum-frequency generation (SFG) to characterize the output of the fiber.[43] If the xFROG is successful, the output of the fiber is properly aligned through the SLM and the wavelengths needed are then reaching the microscope. The uncompressed output of the fiber after the xFROG measurement is shown in Fig 4.7. Compression of the fiber with xFROG has been discussed previously in our lab by Higgins et al.[36] After this measurement is taken and is successful, finding temporal pulse overlap with 400 nm light is another critical piece needed before solution can be placed on the sample stage. This has been the most significant hurdle in switching to a redder probe wavelength. $\beta$-carotene can not be used as a standard solution in this case, because at wavelengths greater than 550 nm, will give a rise to weak or little transient absorption signal.[61, 42] A different standard solution had to be used in order to find our temporal overlap to move on with the study.

The first solution to be attempted was malachite green. The malachite green oxalate salt in water gives great linear absorption at ∼617 nm and at ∼424 nm as shown in Fig 4.8[A]. Its excited state dynamics have been proven in the literature to respond with a pump wavelength of 400 nm and a probe wavelength of 615 nm.[54] A change in solvent from water

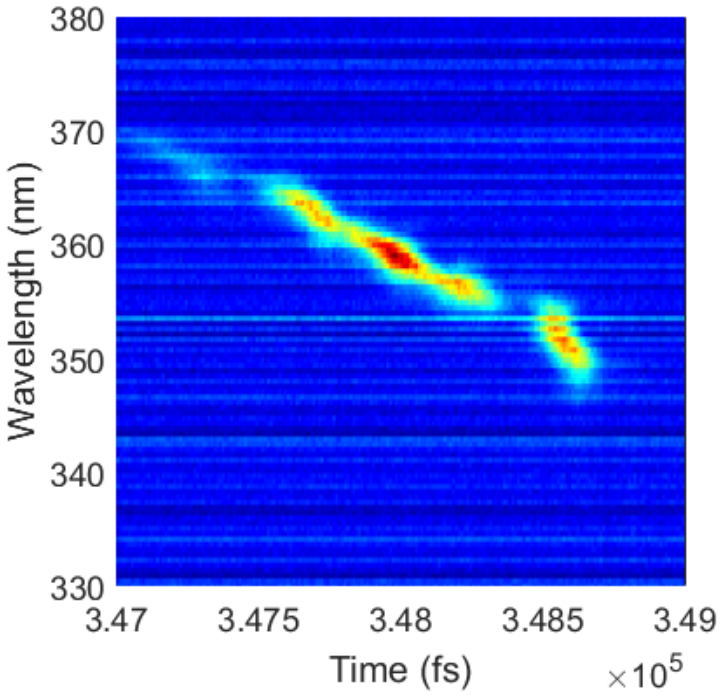


**Figure 4.7:** xFROG spectrum of the Femtowhite 800 and 800 nm light

to ethanol was also attempted with malachite green and has also been previously studied and gives similar linear absorption.[9] However, these results have not been able to be reproduced in the lab. In result of the failed attempts at malachite green, other solutions were to be explored.

The next attempted solution was one of trypan blue, normally used as a cell stain to assess viability. This molecule demonstrates linear absorption at ∼580 nm, but very little at 400 nm as shown in Fig 4.8[B].[15, 29] Studies on the excited state dynamics of trypan blue are non-existent, due to its nature as a cell stain. However, since transient absorption only requires the molecule to absorb light, we went ahead and flowed the solution over our TAM system to attempt use this as a standard for the red-shifted probe wavelengths. This solution was also unsuccessful in the attempts to obtain signal.

After these trials, we decided to go with $\beta$-carotene once again, even though it was previously noted to give weak signal at wavelengths greater than 550 nm.[61, 42] The temporal overlap of the new red-shifted probe wavelength and the 400 nm pump was found with the $\beta$-carotene with a 500 $\mu$M solution in acetone. The spectra of the probe beam used along with the respective TA scan can be seen in Fig 4.9. This data was fit to a

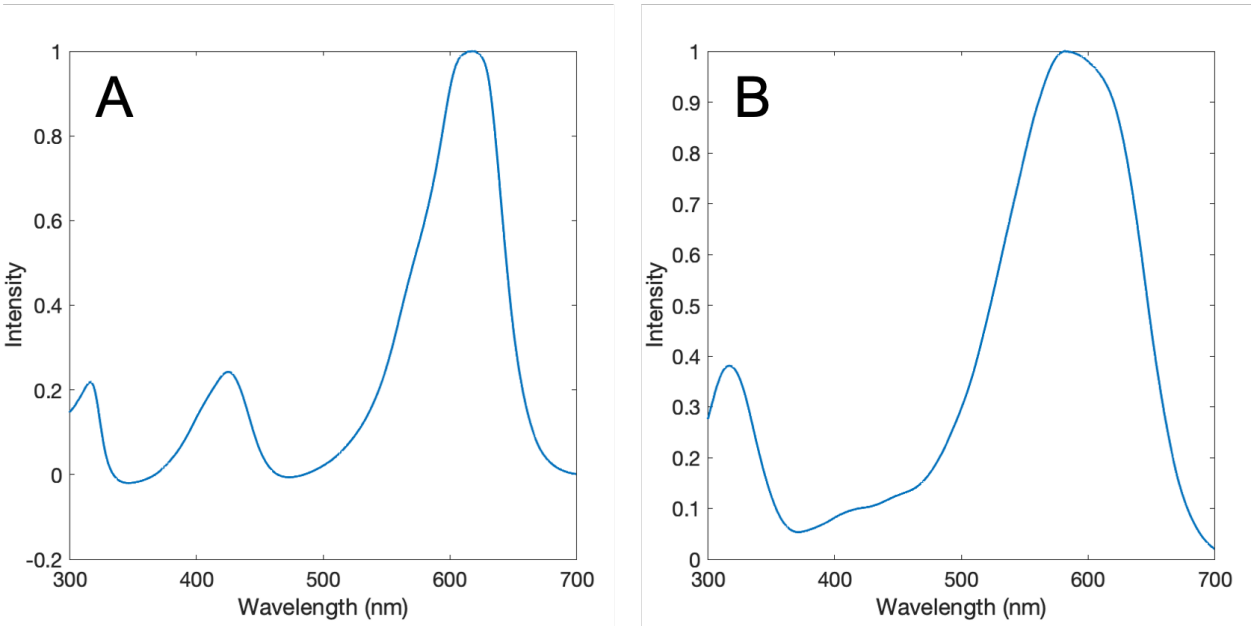


**Figure 4.8:** [A] UV-Vis of 100$\mu$M Malachite Green in water [B] UV-Vis of 100$\mu$M Trypan Blue in water

double exponential from Zewail, et al.[66] and resulted in a shorter component of 0.89 ps and a longer component of 12.9 ps. This result was different than shown in Fig 2.10 due to the red-shifted wavelengths (620-680 nm) used in this scan in comparison to 550 nm used previously. Transient absorption spectroscopy has previously shown that the lifetime of $\beta$-carotene is sensitive due to the difference in the probe wavelength and solvent used.[23] Results from $\beta$-carotene did lead to possible $CS_2$ compression for *that day only* as signal suddenly disappeared with no instrumental changes in the following days.

Because of the issues with using the redder-shifted probe wavelengths, maintenance on the TAM setup was to be completed. Alignment was checked at all positions and iris heights were re-adjusted. There was some drifting of the probe beam as the position changed with the time delay retroreflector which was fixed with alignment. The pump beam was also changing in size as it was traveling through the line. The size change was due to an uncollimated pump beam which stemmed from the off-axis parabolic mirror. It was ultimately concluded that alignment issues were affecting the spatial overlap in the z-dimension into the TA microscope. If the beams are temporally overlapped (in time) but are not perfectly spatially overlapped (including z-dimension), signal can be weak or non-existent as the pulses will not be able to

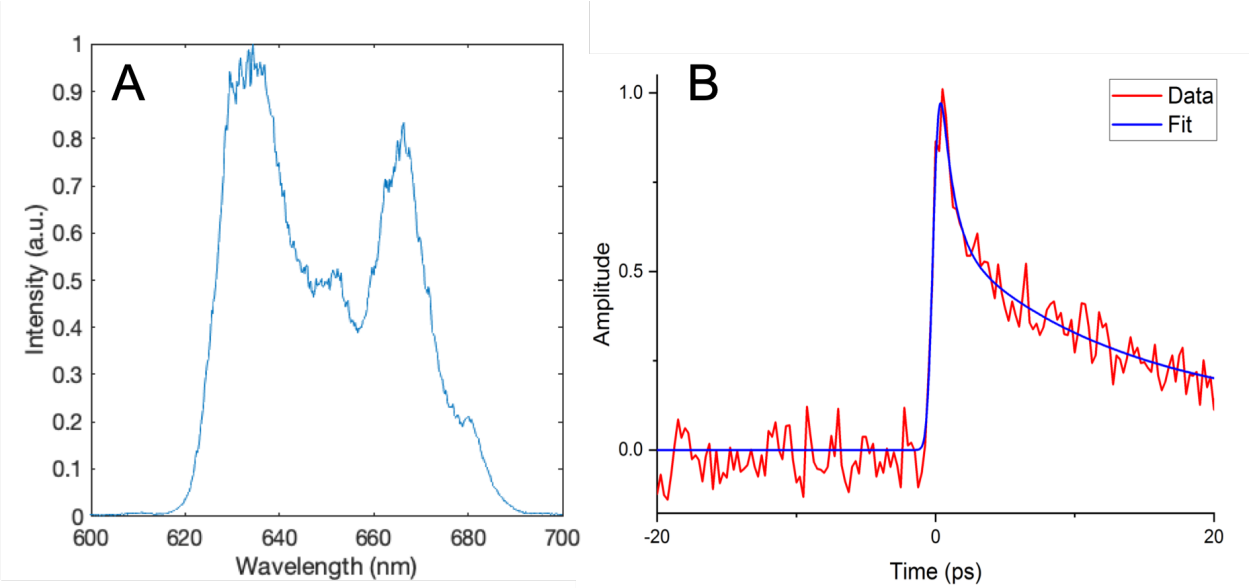


**Figure 4.9:** [A] Spectra of the probe beam used for the TA scan in [B]. [B] TA scan of 500$\mu$M $\beta$-carotene in acetone demonstrating weak signal response utilizing the red-shifted probe wavelengths. Data was fit to a double exponential resulting in a shorter component of 0.89 ps and a longer component of 12.9 ps.

interact with each other. Proper collimation of both beams of light could lead to a better z-dimension overlap, or a re-build of the 400 nm light pump beam setup may need to take place with a swap out of various optics. Ultimately, the collimation of the lines need to be perfected properly. The size of the lenses and the off-axis parabolic mirror may need to be changed and optimized for a better pump beam size down the table. Another issue that may coincide with this and to be adjusted with the 400 nm pump line is the prism size used for compression. The current 400 nm line contains 15 mm SF10 dispersion compensating prisms for compression where the beams both fit, but a 25 mm SF10 prism may allow for more room for alignment and less constraints in the setup. The current prism size allows for the incoming and return beam to fit properly, but with a properly collimated beam the size may be too large for these 15 mm prisms. Having a larger size in the beam line can ease in alignment and collimation, ultimately resulting in finding a better overlap in the z-dimension. A better compound may also need to be used to find t=0 for pulse overlap. However, malachite green and trypan blue may be good candidates when the beam paths are properly orientated into the microscope.

## 4.4 Conclusion

Fungizone is a solution of Amphotericin B that is used commercially to treat those with a life-threatening fungal infection when other methods have failed to help. Due to its availability and functionality, knowing how this widely-used formulation interacts with living fungal systems is crucial. Once more is known of how Fungizone interacts with fungal cells, more specialized treatments could be developed, or even new formulations of Amphotericin B itself. The data obtained at ORNL by Dr. Ma also sheds new light on how aggregated forms of AmB may interact with light differently than monomeric AmB in solution with DMSO.

# Chapter 5

# Conclusions and Future Directions

A new and improved permanent flow cell device was developed and constructed to be used with transient absorption microscopy. The device was used to obtain ultrafast dynamics of molecules in solution and is still being used to this day for that same purpose. The innovation that this device brings will allow for future studies to be completed with TAM on other molecules of interest and can be further improved if necessary. It also aids in our aim of observing drug-membrane interactions on living systems by the ability to observe the flow of drug over cells, as well as in the verification of our pulse compression and instrument response, which is crucial when calculating a lifetime of a sample when studying its dynamics. The development of this device was truly innovative for our lab, for our studies on solutions and to improve on our study of Amphotericin B in both living and model systems.

The studies on Amphotericin B also led to some interesting information on how the drug is interacting with the membranes of fungal systems. From previous to more recent studies, a stable conclusion has not been able to be reached. This leads us to say that the interaction between the living system and Amphotericin B may be impacted by environmental factors and is sensitive to environmental changes. Previous studies have shown what looks like internalization of the drug into the cell, however, recent studies have shown what looks like membrane interactions and no internalization. To come to a clear conclusion of what is occurring here, more control studies need to take place with and without AmB in solution with the media changes and immobilization changes to see if these effects are actually sensitive to the drug's interactions. The model membrane systems are also a good direction

to start modifying the membrane components without the interactions of immobilization methods or media to simply just observe the drug-membrane interactions. The addition of a new method of autofluorescence was also built into the instrument, which will also add in a new way of verification to these new levels of studies which was not available for the media and immobilization change study as discussed in this thesis.

Studies on the Fungizone ® solution were also novel and did yield fascinating results. We were able to replicate the commercial solution with a homemade in-lab solution with a higher concentration of AmB to use in our TAM studies with similar properties as the manufactured solution. We were also able to obtain signal on the solution for the first time with our TAM system using the same conditions that we have used previously for AmB. We then collaborated with Dr. Ma at ORNL who helped us obtain TA data on the solution to optimize our conditions to the proper probe wavelength. This leads us to reason that controlled aggregation of AmB in the micellar-type formation found in Fungizone gives different dynamics than monomeric AmB in solution. We were able to switch our TAM system to a red-shifted PCF which provided the wavelength needed, however, conditions were not sufficient to obtain any applicable data on the solution. Future works are in-place to attempt to obtain signal from this solution with the redder probe wavelengths on the TAM setup.

Overall, a new and robust flow cell device was designed and manufactured and led to progress on studying ultrafast dynamics of various solutions in the lab, and also aided in our goal of imaging drug-membrane interactions *in vivo*. We have also collected more imaging data on AmB's interaction with *S. cerevisiae* which contradicts what was seen before, leaving more questions to be asked, but also possibly suggesting AmB's interaction is environmentally sensitive. Model membrane conditions were also optimized and became more stable due to the protocols established with the Vesicle Prep Pro device and are now more reproducible to be used for future studies. With the help of Dr. Ma at ORNL we now have a clear path to study commercial Fungizone with living systems and could study the difference in interactions with this solution as well. The studies of AmB's mechanism of action are not over yet, but some more light has been shed on what it may be doing to the cells, and why it's been so effective over the past 50 years.

# Bibliography

[1] Alvarez, C., Shin, D. H., and Kwon, G. S. (2016). Reformulation of Fungizone by PEG-DSPE Micelles: Deaggregation and Detoxification of Amphotericin B. *Pharmaceutical research*, 33(9):2098–2106.

[2] Amat-Roldán, I., Cormack, I. G., Loza-Alvarez, P., Gualda, E. J., and Artigas, D. (2004). Ultrashort pulse characterisation with SHG collinear-FROG. *Optics Express*, 12(6):1169–1178.

[3] Anderson, T. M., Clay, M. C., Cioffi, A. G., Diaz, K. A., Hisao, G. S., Tuttle, M. D., Nieuwkoop, A. J., Comellas, G., Maryum, N., Wang, S., Uno, B. E., Wildeman, E. L., Gonen, T., Rienstra, C. M., and Burke, M. D. (2014). Amphotericin forms an extramembranous and fungicidal sterol sponge. *Nature Chemical Biology*, 10(5):400–406.

[4] Austin, D. R., de Sterke, C. M., Eggleton, B. J., and Brown, T. G. (2006). Dispersive wave blue-shift in supercontinuum generation. *Optics Express*, 14(25):11997–12007.

[5] Barrett, J. P., Vardulaki, K. A., Conlon, C., Cooke, J., Daza-Ramirez, P., Evans, E. G. V., Hawkey, P. M., Herbrecht, R., Marks, D. I., Moraleda, J. M., Park, G. R., Senn, S. J., and Viscoli, C. (2003). A systematic review of the antifungal effectiveness and tolerability of amphotericin B formulations. *Clinical Therapeutics*, 25(5):1295–1320.

[6] Bates, D. W., Su, L., Yu, D. T., Chertow, G. M., Seger, D. L., Gomes, D. R. J., Dasbach, E. J., and Platt, R. (2001). Mortality and Costs of Acute Renal Failure Associated with Amphotericin B Therapy. *Clinical Infectious Diseases*, 32(5):686–693.

[7] Bendich, A. and Olson, J. A. (1989). Biological actions of carotenoids. *The FASEB Journal*, 3(8):1927–1932.

[8] Berera, R., van Grondelle, R., and Kennis, J. T. M. (2009). Ultrafast transient absorption spectroscopy: Principles and application to photosynthetic systems. *Photosynthesis Research*, 101(2):105–118.

[9] Bhasikuttan, A. C., Sapre, A. V., and Okada, T. (2003). Ultrafast Relaxation Dynamics from the S2 State of Malachite Green Studied with Femtosecond Upconversion Spectroscopy. *The Journal of Physical Chemistry A*, 107(17):3030–3035.

[10] Bolard, J., Cleary, J. D., and Kramer, R. E. (2009). Evidence that impurities contribute to the fluorescence of the polyene antibiotic amphotericin B. *Journal of Antimicrobial Chemotherapy*, 63(5):921–927.

[11] Bongomin, F., Gago, S., Oladele, R. O., and Denning, D. W. (2017). Global and Multi-National Prevalence of Fungal Diseases—Estimate Precision. *Journal of Fungi*, 3(4).

[12] Botstein, D., Chervitz, S. A., and Cherry, M. (1997). Yeast as a Model Organism. *Science*, 277(5330):1259–1260.

[13] Boyd, M. A. and Kamat, N. P. (2018). Visualizing Tension and Growth in Model Membranes Using Optical Dyes. *Biophysical Journal*, 115(7):1307–1315.

[14] Brajtburg, J., Powderly, W. G., Kobayashi, G. S., and Medoff, G. (1990). Amphotericin B: Current understanding of mechanisms of action. *Antimicrobial Agents and Chemotherapy*, 34(2):183–188.

[15] Brockmann, T., Blanchard, V., Heretsch, P., Brockmann, C., and Bertelmann, E. (2018). Photochemical degradation of trypan blue. *PLoS ONE*, 13(4).

[16] Brown, G. D., Denning, D. W., Gow, N. A. R., Levitz, S. M., Netea, M. G., and White, T. C. (2012). Hidden Killers: Human Fungal Infections. *Science Translational Medicine*, 4(165):165rv13–165rv13.

[17] Chan, Y.-H. M. and Boxer, S. G. (2007). Model Membrane Systems and Their Applications. *Current opinion in chemical biology*, 11(6):581–587.

[18] Cheng, H.-T. and London, E. (2011). Preparation and Properties of Asymmetric Large Unilamellar Vesicles: Interleaflet Coupling in Asymmetric Vesicles Is Dependent on Temperature but Not Curvature. *Biophysical Journal*, 100(11):2671–2678.

[19] Chowdhury, A. U., Watson, B. R., Ma, Y.-Z., Sacci, R. L., Lutterman, D. A., Calhoun, T. R., and Doughty, B. (2019). A new approach to vibrational sum frequency generation spectroscopy using near infrared pulse shaping. *Review of Scientific Instruments*, 90(3):033106.

[20] Clemons, K. V. and Stevens, D. A. (1998). Comparison of Fungizone, Amphotec, AmBisome, and Abelcet for Treatment of Systemic Murine Cryptococcosis. *Antimicrobial Agents and Chemotherapy*, 42(4):899–902.

[21] Davis, J. A., McNamara, D. E., Cottrell, D. M., and Sonehara, T. (2000). Two-dimensional polarization encoding with a phase-only liquid-crystal spatial light modulator. *Applied Optics*, 39(10):1549–1554.

[22] Davydova, D., de la Cadena, A., Akimov, D., and Dietzek, B. (2016). Transient absorption microscopy: Advances in chemical imaging of photoinduced dynamics. *Laser & Photonics Reviews*, 10(1):62–81.

[23] de Weerd, F. L., van Stokkum, I. H. M., and van Grondelle, R. (2002). Subpicosecond dynamics in the excited state absorption of all-trans-$\beta$-Carotene. *Chemical Physics Letters*, 354(1):38–43.

[24] Ermishkin, L. N., Kasumov, K. M., and Potzeluyev, V. M. (1976). Single ionic channels induced in lipid bilayers by polyene antibiotics amphotericin B and nystatine. *Nature*, 262(5570):698–699.

[25] Fittinghoff, D. N., Millard, A. C., Squier, J. A., and Muller, M. (1999). Frequency-resolved optical gating measurement of ultrashort pulses passing through a high numerical aperture objective. *IEEE Journal of Quantum Electronics*, 35(4):479–486.

[26] Galvao, J., Davis, B., Tilley, M., Normando, E., Duchen, M. R., and Cordeiro, M. F. (2013). Unexpected low-dose toxicity of the universal solvent DMSO. *The FASEB Journal*, 28(3):1317–1330.

[27] Gangadhar, K. N., Adhikari, K., and Srichana, T. (2014). Synthesis and evaluation of sodium deoxycholate sulfate as a lipid drug carrier to enhance the solubility, stability and safety of an amphotericin B inhalation formulation. *International Journal of Pharmaceutics*, 471(1):430–438.

[28] González, G. M., Tijerina, R., Najvar, L. K., Bocanegra, R., Rinaldi, M. G., and Graybill, J. R. (2004). Efficacies of Amphotericin B (AMB) Lipid Complex, AMB

Colloidal Dispersion, Liposomal AMB, and Conventional AMB in Treatment of Murine Coccidioidomycosis. *Antimicrobial Agents and Chemotherapy*, 48(6):2140–2143.

[29] Graham, J. P., Rauf, M. A., Hisaindee, S., and Nawaz, M. (2013). Experimental and theoretical study of the spectral behavior of Trypan Blue in various solvents. *Journal of Molecular Structure*, 1040:1–8.

[30] Gray, K. C., Palacios, D. S., Dailey, I., Endo, M. M., Uno, B. E., Wilcock, B. C., and Burke, M. D. (2012). Amphotericin primarily kills yeast by simply binding ergosterol. *Proceedings of the National Academy of Sciences*, 109(7):2234–2239.

[31] Gruszecki, W. I., Gagoś, M., and Hereć, M. (2003). Dimers of polyene antibiotic amphotericin B detected by means of fluorescence spectroscopy: Molecular organization in solution and in lipid membranes. *Journal of Photochemistry and Photobiology. B, Biology*, 69(1):49–57.

[32] Gruszecki, W. I., Luchowski, R., Gagoś, M., Arczewska, M., Sarkar, P., Hereć, M., Myśliwa-Kurdziel, B., Strzałka, K., Gryczynski, I., and Gryczynski, Z. (2009). Molecular organization of antifungal antibiotic amphotericin B in lipid monolayers studied by means of Fluorescence Lifetime Imaging Microscopy. *Biophysical Chemistry*, 143(1):95–101.

[33] Hayden, O., Agarwal, R., and Lieber, C. M. (2006). Nanoscale avalanche photodiodes for highly sensitive and spatially resolved photon detection. *Nature Materials*, 5(5):352–356.

[34] Heidt, A. M., Hartung, A., Bosman, G. W., Krok, P., Rohwer, E. G., Schwoerer, H., and Bartelt, H. (2011). Coherent octave spanning near-infrared and visible supercontinuum generation in all-normal dispersion photonic crystal fibers. *Optics Express*, 19(4):3775–3787.

[35] Higgins, K. (2018). Transient Absorption Microscopy, Instrumentation and Application to Amphotericin B. *Master's Thesis, University of Tennessee*.

[36] Higgins, K. and Calhoun, T. R. (2018). Compressed supercontinuum probe for transient absorption microscopy. *Optics Letters*, 43(8):1750–1753.

[37] Hilligsøe, K. M., Andersen, T. V., Paulsen, H. N., Nielsen, C. K., Mølmer, K., Keiding, S., Kristiansen, R., Hansen, K. P., and Larsen, J. J. (2004). Supercontinuum generation in a photonic crystal fiber with two zero dispersion wavelengths. *Optics Express*, 12(6):1045–1054.

[38] Kandori, H., Sasabe, H., and Mimuro, M. (1994). Direct Determination of a Lifetime of the S2 State of .beta.-Carotene by Femtosecond Time-Resolved Fluorescence Spectroscopy. *Journal of the American Chemical Society*, 116(6):2671–2672.

[39] Karathia, H., Vilaprinyo, E., Sorribas, A., and Alves, R. (2011). Saccharomyces cerevisiae as a Model Organism: A Comparative Study. *PLOS ONE*, 6(2):e16015.

[40] Kołaczkowska, A. and Kołaczkowski, M. (2016). Drug resistance mechanisms and their regulation in non-albicans Candida species. *Journal of Antimicrobial Chemotherapy*, 71(6):1438–1450.

[41] Kumar, V., Rana, K. P. S., Kumar, A., Sharma, R., Mishra, P., and Nair, S. S. (2014). Development of a Genetic Algorithm Toolkit in LabVIEW. In Pant, M., Deep, K., Nagar, A., and Bansal, J. C., editors, *Proceedings of the Third International Conference on Soft Computing for Problem Solving*, Advances in Intelligent Systems and Computing, pages 281–296. Springer India.

[42] Larsen, D. S., Papagiannakis, E., van Stokkum, I. H. M., Vengris, M., Kennis, J. T. M., and van Grondelle, R. (2003). Excited state dynamics of $\beta$-carotene explored with dispersed multi-pulse transient absorption. *Chemical Physics Letters*, 381(5):733–742.

[43] Linden, S., Giessen, H., and Kuhl, J. (1998). XFROG — A New Method for Amplitude and Phase Characterization of Weak Ultrashort Pulses. *physica status solidi (b)*, 206(1):119–124.

[44] McClean, M. (2015). McClean:LFM Recipe. https://openwetware.org/wiki/McClean:LFM_Recipe.

[45] Mishra, N., Prasad, T., Sharma, N., Payasi, A., Prasad, R., Gupta, D., and Singh, R. (2007). Pathogenicity and drug resistance in Candida albicans and other yeast species. *Acta Microbiologica et Immunologica Hungarica*, 54(3):201–235.

[46] Mohanty, J., Palit, D., and Mittal, J. (2000). Photophysical Properties of Two Infrared Laser Dies-IR-144 and IR-140: A Picosecond Laser Flash Photolysis Study. *Proceedings of the Indian National Science Academy*, 66(2A):303–315.

[47] Moore, J. H. (1995). Artificial intelligence programming with LabVIEW: Genetic algorithms for instrumentation control and optimization. *Computer Methods and Programs in Biomedicine*, 47(1):73–79.

[48] Nazir, A. J. A., Gautham, Surajan, R., and Binu, L. S. (2009). A simplified Genetic Algorithm for online tuning of PID controller in LabView. In *2009 World Congress on Nature Biologically Inspired Computing (NaBIC)*, pages 1516–1519.

[49] Neumann, A., Baginski, M., and Czub, J. (2010). How Do Sterols Determine the Antifungal Activity of Amphotericin B? Free Energy of Binding between the Drug and Its Membrane Targets. *Journal of the American Chemical Society*, 132(51):18266–18272.

[50] Odds, F. C., Brown, A. J. P., and Gow, N. A. R. (2003). Antifungal agents: Mechanisms of action. *Trends in Microbiology*, 11(6):272–279.

[51] Pamp, S. J., Sternberg, C., and Tolker-Nielsen, T. (2009). Insight into the microbial multicellular lifestyle via flow-cell technology and confocal microscopy. *Cytometry Part A*, 75A(2):90–103.

[52] Patterson, G. H. and Piston, D. W. (2000). Photobleaching in Two-Photon Excitation Microscopy. *Biophysical Journal*, 78(4):2159–2162.

[53] Peter, J., Armstrong, D., Lyman, C. A., and Walsh, T. J. (2005). Use of Fluorescent Probes To Determine MICs of Amphotericin B and Caspofungin against Candida spp. and Aspergillus spp. *Journal of Clinical Microbiology*, 43(8):3788–3792.

[54] Punzi, A., Martin-Gassin, G., Grilj, J., and Vauthey, E. (2009). Effect of Salt on the Excited-State Dynamics of Malachite Green in Bulk Aqueous Solutions and at Air/Water Interfaces: A Femtosecond Transient Absorption and Surface Second Harmonic Generation Study. *The Journal of Physical Chemistry C*, 113(27):11822–11829.

[55] Reichert, M., Hu, H., Ferdinandus, M. R., Seidel, M., Zhao, P., Ensley, T. R., Peceli, D., Reed, J. M., Fishman, D. A., Webster, S., Hagan, D. J., and Stryland, E. W. V. (2014). Temporal, spectral, and polarization dependence of the nonlinear optical response of carbon disulfide. *Optica*, 1(6):436–445.

[56] Sánchez, E. J., Novotny, L., Holtom, G. R., and Xie, X. S. (1997). Room-Temperature Fluorescence Imaging and Spectroscopy of Single Molecules by Two-Photon Excitation. *The Journal of Physical Chemistry A*, 101(38):7019–7023.

[57] Scofield, J. H. (1994). Frequency-domain description of a lock-in amplifier. *American Journal of Physics*, 62(2):129–133.

[58] Seybold, P. G., Gouterman, M., and Callis, J. (1969). Calorimetric, Photometric and Lifetime Determinations of Fluorescence Yields of Fluorescein Dyes. *Photochemistry and Photobiology*, 9(3):229–242.

[59] Sokol-Anderson, M. L., Brajtburg, J., and Medoff, G. (1986). Amphotericin B-induced oxidative damage and killing of Candida albicans. *The Journal of Infectious Diseases*, 154(1):76–83.

[60] Su, H., Han, L., and Huang, X. (2018). Potential targets for the development of new antifungal drugs. *The Journal of Antibiotics*.

[61] Vdović, S., Wang, Y., Li, B., Qiu, M., Wang, X., Guo, Q., and Xia, A. (2013). Excited state dynamics of $\beta$-carotene studied by means of transient absorption spectroscopy and multivariate curve resolution alternating least-squares analysis. *Physical Chemistry Chemical Physics*, 15(46):20026–20036.

[62] Vermes, A., Guchelaar, H.-J., and Dankert, J. (2000). Flucytosine: A review of its pharmacology, clinical indications, pharmacokinetics, toxicity and drug interactions. *Journal of Antimicrobial Chemotherapy*, 46(2):171–179.

[63] Weiner, A. M. (2000). Femtosecond pulse shaping using spatial light modulators. *Review of Scientific Instruments*, 71(5):1929–1960.

[64] Ye, T., Fu, D., and Warren, W. S. (2009). Nonlinear Absorption Microscopy†. *Photochemistry and Photobiology*, 85(3):631–645.

[65] Zeidler, D. (2001). Coherent Control of Molecular Dynamics with Shaped Femtosecond Pulses. *Doctoral Dissertation, der Ludwig-Maximilians-Universitat Munchen.*

[66] ZEWAIL, S. P. A. H. (1996). Femtosecond real time probing of reactions XXII Kinetic description of probe absorption fluorescence depletion and mass spectrometry. *Molecular Physics*, 89(5):1455–1502.

[67] Zumbuehl, A., Jeannerat, D., Martin, S. E., Sohrmann, M., Stano, P., Vigassy, T., Clark, D. D., Hussey, S. L., Peter, M., Peterson, B. R., Pretsch, E., Walde, P., and Carreira, E. M. (2004). An Amphotericin B–Fluorescein Conjugate as a Powerful Probe for Biochemical Studies of the Membrane. *Angewandte Chemie International Edition*, 43(39):5181–5185.

# Vita

Brandon Woitas was born and raised in Buffalo, New York to Paul and Josephine Woitas. Brandon attended The State University of New York College at Buffalo (SUNY Buffalo State) where he earned a Bachelor of Science degree in Forensic Chemistry in 2017. During his time there, he performed undergraduate research under the guidance of Dr. Alexander Nazarenko. Brandon then was accepted to The University of Tennessee, Knoxville, where he would dive into the world of ultrafast laser spectroscopy to pursue a graduate degree in chemistry under the guidance of Dr. Tessa Calhoun.